

Supporting Information

Isolation, Structure Elucidation and Racemization of (+)- and (−)-Pratensilins A–C, Unprecedented Spiro Indolinone-naphthofuran Alkaloids from a Marine *Streptomyces* sp.

Authors: Shumin Zhang,^a Qin Yang,^a Lin Guo,^a Ying Zhang,^b Lingling Feng,^a Ling Zhou,^a Shengxiang Yang,^c Qingshou Yao,^a Gennaro Pescitelli*,^d and Zeping Xie*,^a

^aSchool of Pharmacy, ^bSchool of Basic Medical Sciences, Binzhou Medical University, Yantai 264003, China

^cKey Laboratory of Chemical Utilization of Forestry Biomass of Zhejiang Province, Zhejiang A&F University, Lin'an, Zhejiang 311300, China

^dDipartimento di Chimica e Chimica Industriale, Università di Pisa, Via Moruzzi 13, 56124 Pisa, Italy

Contents

General experimental procedures	6
Collection and phylogenetic analysis of strain KCB-132	6
Cultivation and culture extraction	6
Isolation of pratensilins A-C (1-3)	7
Methyl pratensilin B (4):	8
Computational section	9
Cytotoxicity bioassay	10
Table S1. NMR data for (\pm)-pratensilin A (1) in DMSO- <i>d</i> ₆ ^a	10
Table S2. NMR data for (\pm)-pratensilin B (2) in DMSO- <i>d</i> ₆ ^a	11
Table S3. NMR data for (\pm)-pratensilin C (3) in DMSO- <i>d</i> ₆ ^a	13
Table S4. Cytotoxicities of compounds 1-4	15
Fig. S1 X-ray crystal structure of 2	16
Fig. S2 X-ray crystal structure of 3	17
Fig. S3 Experimental and calculated ECD spectra for (+)-(S)- 3 and (-)-(R)- 3	18

Fig. S4 Torsional energy scans around the biaryl axis computed at B97X-DD/6-31G(d,p) level. Plotted energy relative to compound 2	19
Fig. S5 Torsional energy scans around the biaryl axis computed at B97X-DD/6-31G(d,p) level. Plotted energy relative to compound 3	20
Fig. S6 ^1H NMR spectrum (500 MHz) of (\pm)-pratensilin A (1) in DMSO- d_6	21
Fig. S7 ^{13}C NMR spectrum (125 MHz) of (\pm)-pratensilin A (1) in DMSO- d_6	22
Fig. S8 DEPT-135 spectrum (125 MHz) of (\pm)-pratensilin A (1) in DMSO- d_6	23
Fig. S9 COSY spectrum (500 MHz) of (\pm)-pratensilin A (1) in DMSO- d_6	24
Fig. S10 HSQC spectrum (500 MHz) of (\pm)-pratensilin A (1) in DMSO- d_6	25
Fig. S11 HMBC spectrum (500 MHz) of (\pm)-pratensilin A (1) in DMSO- d_6	26
Fig. S12 NOESY spectrum (500 MHz) of (\pm)-pratensilin A (1) in DMSO- d_6	27
Fig. S13 HRESIMS spectrum of (\pm)-pratensilin A (1).....	28
Fig. S14 UV spectrum of (+)-pratensilin A ((+)- 1).....	29
Fig. S15 UV spectrum of (-)-pratensilin A ((-)- 1).....	30
Fig. S16 IR spectrum of (\pm)-pratensilin A (1).....	31
Fig. S17 ^1H NMR spectrum (500 MHz) of (\pm)-pratensilin B (2) in DMSO- d_6	32
Fig. S18 ^{13}C NMR spectrum (125 MHz) of (\pm)-pratensilin B (2) in DMSO- d_6	33
Fig. S19 DEPT-135 spectrum (125 MHz) of (\pm)-pratensilin B (2) in DMSO- d_6	34
Fig. S20 COSY spectrum (500 MHz) of (\pm)-pratensilin B (2) in DMSO- d_6	35
Fig. S21 HSQC spectrum (500 MHz) of (\pm)-pratensilin B (2) in DMSO- d_6	36

Fig. S22 HMBC spectrum (500 MHz) of (\pm)-pratensilin B (2) in DMSO- <i>d</i> ₆	37
Fig. S23 NOESY spectrum (500 MHz) of (\pm)-pratensilin B (2) in DMSO- <i>d</i> ₆	38
Fig. S24 HRESIMS spectrum of (\pm)-pratensilin B (2).....	39
Fig. S25 UV spectrum of (+)-pratensilin B ((+)- 2)	40
Fig. S26 UV spectrum of (-)-pratensilin B ((-)- 2)	41
Fig. S27 IR spectrum of (\pm)-pratensilin B (2)	42
Fig. S28 ¹ H NMR spectrum (500 MHz) of (\pm)-pratensilin C (3) in DMSO- <i>d</i> ₆	43
Fig. S29 ¹³ C NMR spectrum (125 MHz) of (\pm)-pratensilin C (3) in DMSO- <i>d</i> ₆	44
Fig. S30 DEPT-135 spectrum (125 MHz) of (\pm)-pratensilin C (3) in DMSO- <i>d</i> ₆	45
Fig. S31 COSY spectrum (500 MHz) of (\pm)-pratensilin C (3) in DMSO- <i>d</i> ₆	46
Fig. S32 HSQC spectrum (500 MHz) of (\pm)-pratensilin C (3) in DMSO- <i>d</i> ₆	47
Fig. S33 HMBC spectrum (500 MHz) of (\pm)-pratensilin C (3) in DMSO- <i>d</i> ₆	48
Fig. S34 NOESY spectrum (500 MHz) of (\pm)-pratensilin C (3) in DMSO- <i>d</i> ₆	49
Fig. S35 HRESIMS spectrum of (\pm)-pratensilin C (3).....	50
Fig. S36 UV spectrum of (+)-pratensilin C ((+)- 3)	51
Fig. S37 UV spectrum of (-)-pratensilin C ((-)- 3)	52
Fig. S38 IR spectrum of (\pm)-pratensilin C (3)	53
Fig. S39 ¹ H NMR spectrum (500 MHz) of (\pm)-methy pratensilin B (4) in DMSO- <i>d</i> ₆	54

Fig. S40 ^{13}C NMR spectrum (125 MHz) of (\pm)-methy pratensilin B (4) in $\text{DMSO}-d_6$	55
Fig. S41 ESIMS spectrum of (\pm)-methy pratensilin B (4)	56
Fig. S42 UV spectrum of (+)-methy pratensilin B ((+)- 4)	57
Fig. S43 UV spectrum of (-)-methy pratensilin B ((-)- 4)	58
Fig. S44 ^1H NMR spectrum (500 MHz) of 8- <i>O</i> -methylrabelomycin in CDCl_3	59
Fig. S45 ^{13}C NMR spectrum (125 MHz) of 8- <i>O</i> -methylrabelomycin in CDCl_3	60
Fig. S46 ESIMS spectrum of 8- <i>O</i> -methylrabelomycin.....	61
Table S5. Crystal data and structure refinement for (\pm)-pratensilins A (1).....	62
Table S6. Crystal data and structure refinement for (\pm)-pratensilins B (2).....	64
Table S7. Crystal data and structure refinement for (\pm)-pratensilins C (3).....	66

General experimental procedures. Optical rotations were measured by a JASCO P-1020 digital polarimeter. UV spectra were recorded by a Shimadzu UV-2401PC spectrometer. CD spectra were recorded using a JASCO J-810 spectropolarimeter. IR spectra were recorded on a Thermo NICOLET IS10 spectrometer. ¹H and 2D NMR spectra were measured at 500 MHz in DMSO-*d*₆ by a Bruker AVANCE IIITM 500 spectrometer, and ¹³C NMR spectra were acquired at 125.8 MHz, the chemical shifts were referenced to DMSO-*d*₆ (δ_{H} 2.50/ δ_{C} 39.99). ESI-MS were performed through a Finnigan LCQ with quaternary pump Rheos 4000 (Flux Instrument). ESI-HRMS were recorded on an Agilent G6230 TOF spectrometer. Single crystal X-ray crystallography was determined on SMART APEX II DUO X-ray single crystal diffractometer using Cu K α radiation. Preparative HPLC was performed on a Waters 2489 series instrument with a UV/Visible detector, using a reversed-phase C₁₈ column (Phenomenex, 250 × 21.2 mm, 5 μm). Chiral HPLC was carried out on an Agilent 1260 liquid chromatograph, utilized chiral analytical columns [(R,R) WHELK-01 column, 4.6×250 mm, 10 μm , 100 Å]. TLC and column chromatography were performed on plates precoated with silica gel GF254 (10–40 μm) and over silica gel (200–300 mesh, Yantai Chemical Industry Institute, Yantai, China).

Collection and phylogenetic analysis of strain KCB-132. *Streptomyces* sp. strain KCB-132 was isolated from a sediment sample collected off the Bohai Sea, China. The sediment was desiccated and stamped onto agar plates using Gause's synthetic media (20 g starch, 1 g KNO₃, 0.5 g K₂HPO₄, 0.5 g MgSO₄·7H₂O, 0.01 g FeSO₄·7H₂O, 0.3 g K₂Cr₂O₇, seawater 500 mL, deionized water 500 mL, pH 7.4). Analysis of the strain by 16S rRNA revealed 99.93% identity to *Streptomyces pratensis*. The sequence is deposited in GenBank under accession no. KX033803.

Cultivation and culture extraction. *Streptomyces* strain KCB-132 was initially cultured in 200 mL of ISP2 medium (pH 7.8±0.2) in 1 L flask for 48 h at 28 °C, and then were inoculated to 54 L (250 mL × 216) seawater-based ISP2 medium (5 g of malt extract, 4 g of yeast extract, 4 g of glucose, 500 mL of deionized water and 500 mL of seawater, pH 7.8±0.2) for 10 days at 28 °C. The culture broth was filtered to provide filtrate

and mycelium. The filtrate was absorbed onto XAD-16 amberlite resin, and the resin was extracted with methanol, then dry out methanol under reduced pressure to give the crude extract, which was resolved in 1 L of H₂O, the water phase was extracted with ethyl acetate, and the mycelium was extracted by ethyl acetate under ultrasonic radiation directly, both ethyl acetate phase were combined to give 8.1 g extract materials.

Isolation of pratensilins A-C (1-3). The extract (8.1 g) was fractioned using silica gel column chromatography (CC) and eluted with CH₂Cl₂-MeOH gradient system (100:0, 99:1, 95:5, 90:10, 80:20, 50:50, and 0:100, v/v) to yield seven fractions (Fr.A-Fr.G). Fr.C (3.3 g) was subjected to ODS CC with a stepwise gradient of MeOH-H₂O (10:90→100:0) to provide ten fractions (Fr.C1-Fr.C10), and Fr.C7 (730 mg) was purified by reversed-phase HPLC (Phenomenex Luna, C₁₈, 250 × 21.2 mm, 5 μm, 10 mL/min, UV = 210 nm) eluting with 60% MeOH in H₂O to afford (±)-pratensilin A (**1**, 5.5 mg, *t*_R = 44.9 min), and Fr.C8 (560 mg) was purified by reversed-phase HPLC (55% MeOH/H₂O) to give (±)-pratensilin B (**2**, 12.2 mg, *t*_R = 32.1 min) and (±)-pratensilin C (**3**, 4.1 mg, *t*_R = 36.9 min). Chiral separation of **1** was performed on Agilent analytical HPLC system ((R,R) WHELK-01 column, 4.6×250 mm, 10 μm, 100 Å, acetone/n-hexane = 40:60, 1.0 mL/min, UV = 210 nm) to afford optically pure (+)-**1** (2.2 mg, *t*_R = 3.9 min) and (-)-**1** (2.2 mg, *t*_R = 4.6 min), the racemic mixture of **2** was separated on 30% acetone/n-hexane to afford (+)-**2** (0.9 mg, *t*_R = 7.2 min) and (-)-**2** (0.9 mg, *t*_R = 8.0 min), and **3** was purified on 12% acetone/n-hexane to yield (-)-**3** (0.6 mg, *t*_R = 16.4 min) and (+)-**3** (0.6 mg, *t*_R = 17.5 min).

(+)-Pratensilin A ((+)-1): colorless solid; $[\alpha]_D^{25} + 7.3$ (Acetone, *c* 0.11); UV (Acetonitrile) $\Delta\lambda_{\max}$ (log ε) 210 (3.7), 243 (3.4), 302 (2.7), 345 (2.1) nm; IR (ATR) ν_{\max} 3518, 3383, 3209, 2921, 2846, 1683, 1608, 1487, 1273, 1257, 1099, 795 cm⁻¹; 1D and 2D-NMR (500 MHz, DMSO-*d*₆), see Table S1; HRESIMS [M+Na]⁺, *m/z* 356.0895 (Δ -0.4 ppm).

(-)-Pratensilin A ((-)-1): colorless solid; $[\alpha]_D^{25} - 34.6$ (Acetone, *c* 0.04); UV (Acetonitrile) $\Delta\lambda_{\max}$ (log ε) 210 (3.8), 242 (3.4), 302 (2.7), 342

(2.2) nm; IR (ATR) ν_{max} 3518, 3383, 3209, 2921, 2846, 1683, 1608, 1487, 1273, 1257, 1099, 795 cm⁻¹; 1D and 2D-NMR (500 MHz, DMSO-*d*₆), see Table S1; HRESIMS [M+Na]⁺, *m/z* 356.0895 (Δ -0.4 ppm).

(+)-Pratensilin B ((+)-2): colorless solid; $[\alpha]_D^{25} + 13.3$ (Acetone, *c* 0.11); UV (Acetonitrile) λ_{max} (log ε) 212 (3.9), 242 (3.7), 301 (2.9), 342 (2.5) nm; IR (ATR) ν_{max} 3376, 3241, 2917, 1703, 1672, 1611, 1487, 1257, 1122, 1052, 947, 745; 1D and 2D-NMR (500 MHz, DMSO-*d*₆), see Table S2; HRESIMS [M+H]⁺, *m/z* 334.1075 (Δ 1.3 ppm).

(-)-Pratensilin B ((-)-2): colorless solid; $[\alpha]_D^{25} - 53.3$ (Acetone, *c* 0.04); UV (Acetonitrile) λ_{max} (log ε) 210 (3.9), 242 (3.7), 302 (2.8), 342 (2.4) nm; IR (ATR) ν_{max} 3376, 3241, 2917, 1703, 1672, 1611, 1487, 1257, 1122, 1052, 947, 745; 1D and 2D-NMR (500 MHz, DMSO-*d*₆), see Table S2; HRESIMS [M+H]⁺, *m/z* 334.1075 (Δ 1.3 ppm).

(+)-Pratensilin C ((+)-3): colorless solid; $[\alpha]_D^{25} + 10.0$ (Acetonitrile, *c* 0.03); UV (Acetonitrile) λ_{max} (log ε) 213 (3.6), 242 (3.4), 300 (2.6), 343 (2.2) nm; IR (ATR) ν_{max} 2919, 2847, 1611, 1390, 1247, 1212, 1063, 1011, 829, 753; 1D and 2D-NMR (500 MHz, DMSO-*d*₆), see Table S3; HRESIMS [M+Na]⁺, *m/z* 376.1190 (Δ 0.7 ppm).

(-)-Pratensilin C ((-)-3): colorless solid; $[\alpha]_D^{25} - 63.6$ (Acetonitrile, *c* 0.04); UV (Acetonitrile) λ_{max} (log ε) 213 (3.5), 242 (3.4), 301 (2.6), 344 (2.3) nm; IR (ATR) ν_{max} 2919, 2847, 1611, 1390, 1247, 1212, 1063, 1011, 829, 753; 1D and 2D-NMR (500 MHz, DMSO-*d*₆), see Table S3; HRESIMS [M+Na]⁺, *m/z* 376.1190 (Δ 0.7 ppm).

Notice: the values of optical rotations are only approximate due to the low amount used in the measurements, contamination with the optical antipode or a chiral impurity not detectable at NMR.

Methyl pratensilin B (4): To a solution of pratensilin B (**2**) (2.3 mg, 0.007 mmol) in dry tetrahydrofuran (3.0 mL) at room temperature was added potassium carbonate (19 mg, 0.14 mmol) followed by dimethyl sulfate (0.9 μ L, 0.0105 mmol). The mixture was stirred at room temperature overnight, then diluted with water (10 mL) and extracted with EtOAc (3 x 5 mL). The combined extracts were dried, filtered, and

concentrated, and the product was purified by reversed-phase HPLC (80% MeOH in water, $t_R = 10.57$ min, Phenomenex Luna, C₁₈, 250 × 21.2 mm, 5 μm, 10 mL/min, UV = 210 nm) to give 1.8 mg (75%) of **4** as a light pink solid; ¹H NMR (500 MHz, DMSO-*d*₆) δ 9.54 (s) 7.78 (d, *J* = 8.9 Hz), 7.59 (t, *J* = 7.9 Hz), 7.36 (d, *J* = 7.9 Hz), 7.35 (d, *J* = 8.9 Hz), 7.20 (d, *J* = 7.9 Hz), 7.13 (s), 6.58 (s), 3.66 (s), 3.39 (s), 2.46 (s); ¹³C NMR (125 MHz, DMSO-*d*₆) δ 168.4, 157.5, 155.6, 150.7, 137.0, 133.3, 132.9, 130.9, 128.5, 127.4, 126.2, 118.9, 117.0, 116.4, 115.2, 115.1, 103.3, 101.1, 56.8, 56.3, 22.9. The enantioseparation of the racemic mixture of (±)-**4** was achieved by chiral HPLC (50% isopropanol/n-hexane, (R,R) WHELK-01 column, 4.6 × 250 mm, 10 μm, 100 Å, UV = 210 nm) to yield (+)-**4** (0.8 mg, $t_R = 13.8$ min) and (−)-**4** (0.8 mg, $t_R = 17.8$ min).

(+)-Methy pratensilin B ((+)-4): light pink solid; $[\alpha]_D^{25} + 8.5$ (MeOH, *c* 0.1); UV (MeOH) λ_{\max} (log ε) 211 (3.4), 244 (3.3), 304 (2.4), 345 (1.9) nm; HRESIMS [M+H]⁺, *m/z* 348.1235 (Δ 0.2 ppm).

(−)-Methy pratensilin B ((−)-4): colorless solid; $[\alpha]_D^{25} - 35.8$ (MeOH, *c* 0.1); UV (MeOH) λ_{\max} (log ε) 211 (3.4), 243 (3.4), 304 (2.5), 342 (2.0) nm; HRESIMS [M+H]⁺, *m/z* 348.1235 (Δ 0.2 ppm).

Computational section. MMFF and DFT calculations were run with Spartan'14 (Wavefunction, Inc., Irvine CA, 2014), with standard parameters and convergence criteria. TDDFT calculations were run with Gaussian'09 (Rev. D.01, Gaussian, Inc., Wallingford CT, 2013), with default grids and convergence criteria. Conformational searches were run with the Monte Carlo algorithm implemented in Spartan'14 using Merck molecular force field (MMFF). All structures thus obtained were first optimized with DFT method using ωB97X-D functional and 6-31G(d) basis set in vacuo, and then re-optimized using ωB97X-D functional and 6-31G(d,p) basis set. Torsional energy scans were run by varying the dihedral angle relative to the biaryl axis by 10° steps; calculations were run at B97X-D/6-31G(d,p) level. TDDFT calculations were run using ωB97X-D functional and def2TZVP basis set, including 36 excited states. On some selected structures of compound **1**, other functionals (B3LYP, CAM-B3LYP, BH&HLYP) and basis sets (SVP) were also tested, leading to consistent results. ECD spectra were generated using the program SpecDis (v. 1.70, T. Bruhn, A. Schaumlöffel, Y. Hemberger, G. Pescitelli, Berlin, Germany, 2017, <https://specdis>

software.jimdo.com/), by applying a Gaussian band shape with 0.25-0.3 eV exponential half-width, from dipole-length rotational strengths. Boltzmann populations were estimated at 300K from internal energies calculated at ωB97X-D/def2TZVP level. For each compound, all conformers with Boltzmann population >1% at 300K were included in the calculations. They amounted to 3 conformers for compound **1**, 2 for **2**, and 10 for **3**, respectively. In the final comparison with experimental spectra a wavelength correction of +20 nm, and scaling factors of 2-2.5 were employed.

Cytotoxicity bioassay. The PANC-1 (pancreatic cancer), JHH-7 (hepatocellular carcinoma), C6 (glioma) and HepG2 (hepatocellular carcinoma) cells were plated at a density of 5000 cells/well in 100 μ L DMEM medium, while NCI-H1975 (non-small cell lung cancer), NCI-H460 (non-small cell lung cancer), A549 (non-small cell lung cancer) and THP-1 (acute monocytic leukemia) cells were plated at a density of 5000 cells/well in 100 μ L 1640 medium. All cell lines were incubated overnight then treated with various concentrations of purified compounds in triplicate. After cultured for 72 h, 20 μ L/well of MTT solution (5 mg/mL, Sigma-Aldrich, USA) was added to each well, plate was cultured for 4 h at 37 °C in a 5% CO₂ atmosphere, which was followed by adding 150 μ L DMSO to dissolve the formazan crystals, and shaking for 5 min. The absorbance was recorded at 570 nm by a microplate Reader. IC₅₀ value was taken using Graph pad Prism 5 software.

Table S1. NMR data for (\pm)-pratensilin A (1**) in DMSO-*d*₆^a**

position	δ_{H} mult (J, Hz)	δ_{C}^b	HMBC	COSY	NOE
1		156.8, C			
2	6.55, s	103.5, CH	1, 4, 8a, 16	4, 16	16
3		136.0, C			
4	7.08, s	115.4, CH	1, 2, 4a, 8a, 16	2, 16	16

4a		125.3, C				
5	7.63, d (8.6)	127.2, CH	1, 4, 7, 8a	6	6	
6	7.10, d (8.6)	121.5, CH	4a, 7, 8, 9	5	5	
7		149.3, C				
7-OH	9.84, s		6, 7, 8			
8		116.2, C				
8a		128.5, C				
9		101.6, C				
10-NH	9.25, s		9, 11, 11a, 15a			
11		167.4, C				
11a		117.4, C				
12		157.0, C				
13	7.15, d (7.9)	113.7, CH	11, 11a, 12, 15	14, 17	14, 17	
14	7.48, t (7.9)	135.3, CH	12, 13, 15a	13, 15	13, 15	
15	6.58, d (7.9)	114.9, CH	9, 11a, 13	14	14	
15a		147.8, C				
16	2.42, s	22.8, CH ₃	2, 3, 4	2, 4	2, 4	
17	3.91, s	56.2, CH ₃	12	13	13	

^a500 MHz for ¹H NMR and 125 MHz for ¹³C NMR. ^bNumbers of attached protons were determined by analysis of 2D spectra.

Table S2. NMR data for (\pm)-pratensilin B (2) in DMSO-*d*₆^a

position	δ_{H} mult (<i>J</i> , Hz)	δ_{C}^b	HMBC	COSY	NOE
1		157.4, C			
2	6.52, s	103.1, CH	1, 4, 8a, 16	4, 16	16
3		135.6, C			
4	7.05, s	115.2, CH	1, 2, 3, 4a, 8a, 16	2, 16	16
4a		125.3, C			
5	7.59, d (8.6)	126.8, CH	4, 4a, 6, 7, 8a	6	6
6	7.06, d (8.6)	121.2, CH	4a, 7, 8, 9	5	5, 7-OH
7		148.8, C			
7-OH	9.68, s		6, 7, 8		6
8		116.1, C			
8a		128.8, C			
9		101.3, C			
10-NH	9.48, s		9, 11, 11a, 15a		
11		168.4, C			
11a		133.5, C			
12	7.34, d (7.9)	115.1, CH	11, 14, 15a	13	13
13	7.58, t (7.9)	132.7, CH	11a, 15	12, 14	12, 14
14	7.19, d (7.9)	116.2, CH	9, 12, 15, 15a	13, 17	13, 17

15		155.6, C			
15a		131.0, C			
16	2.43, s	22.8, CH ₃	2, 3, 4	2, 4	2, 4
17	3.40, s	56.3, CH ₃	15	14	14

^a500 MHz for ¹H NMR and 125 MHz for ¹³C NMR. ^bNumbers of attached protons were determined by analysis of 2D spectra.

Table S3. NMR data for (\pm)-pratensilin C (3) in DMSO-*d*₆^a

position	δ_{H} mult (<i>J</i> , Hz)	δ_{C}^b	HMBC	COSY	NOE
1		157.2, C			
2	6.60, s	103.5, CH	1, 4, 8a, 16	4, 16	16
3		135.9, C			
4	7.11, s	115.8, CH	2, 8a, 16	2, 16	16
4a		125.4, C			
5	7.66, d (8.6)	127.6, CH	1, 4 , 7, 8a	6	6
6	7.09, d (8.6)	121.2, CH	4a, 8	5	5, 7-OH
7		149.2, C			
7-OH	9.80, s		6, 7, 8		6, 19-OH
8		113.9, C			
8a		129.2, C			
9		103.8, C			
11		166.8, C			

11a		132.5, C				
12	7.38, d (7.9)	115.1, CH	11, 14, 15a	13	13	
13	7.60, t (7.9)	132.8, CH	11a, 15	12, 14	12, 14	
14	7.21, d (7.9)	116.5, CH	9, 12, 15, 15a	13, 17	13, 17	
15		155.4, C				
15a		129.6, C				
16	2.45, s	22.8, CH ₃	2, 3, 4	2, 4	2, 4	
17	3.39, s	56.4, CH ₃	15	14	14	
18	2.84-2.89, m 3.17-3.33, m	41.5, CH ₂	9, 11, 19	19	19	
19	3.17-3.33, m	58.8, CH ₂	18	18, 19-OH	18, 19-OH	
19-OH	4.60, t (5.6)		18, 19	19	7-OH, 19	

^a500 MHz for ¹H NMR and 125 MHz for ¹³C NMR. ^bNumbers of attached protons were determined by analysis of 2D spectra.

Table S4. Cytotoxicities of compounds 1–4.

Cell line	IC ₅₀ (μM)					
	1	2	(S)-3	(R)-3	(S)-4	(R)-4
NCI-H1975	18.4	50.1			>100	50.8
NCI-H460	31.4	53.2			2.4	6.3
JHH-7	43.9	>100			18.4	82.7
C6	44.3	76.7			61.9	35.0
A549	>100	>100	>100	>100	22.4	31.1
THP-1	67.4	84.8	71.7	53.7	13.9	32.1
PANC-1	>100	>100	>100	>100	42.0	>100
HepG2	50.3	>100	>100	>100	9.0	>100

Fig. S1 X-ray crystal structure of **2**.



Fig. S2 X-ray crystal structure of **3**.

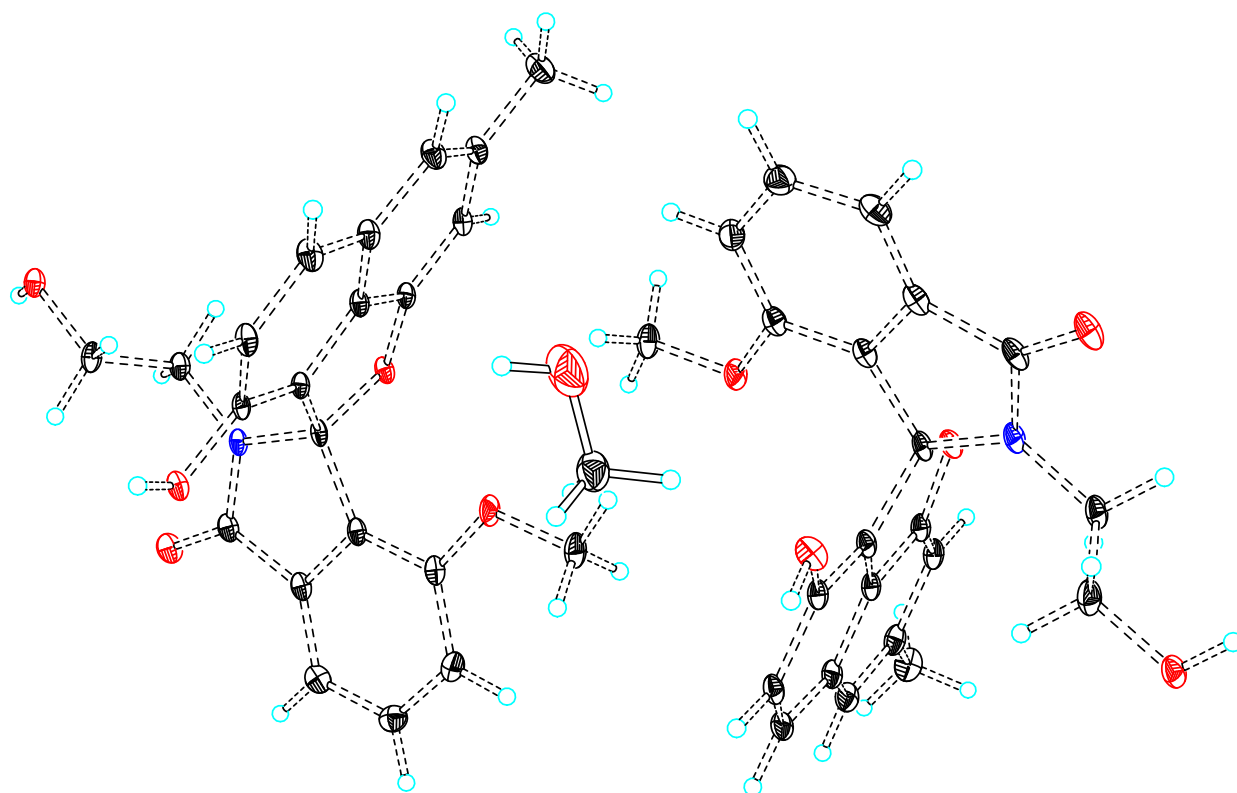


Fig. S3 Experimental and calculated ECD spectra for (+)-(S)-3 and (-)-(R)-3.

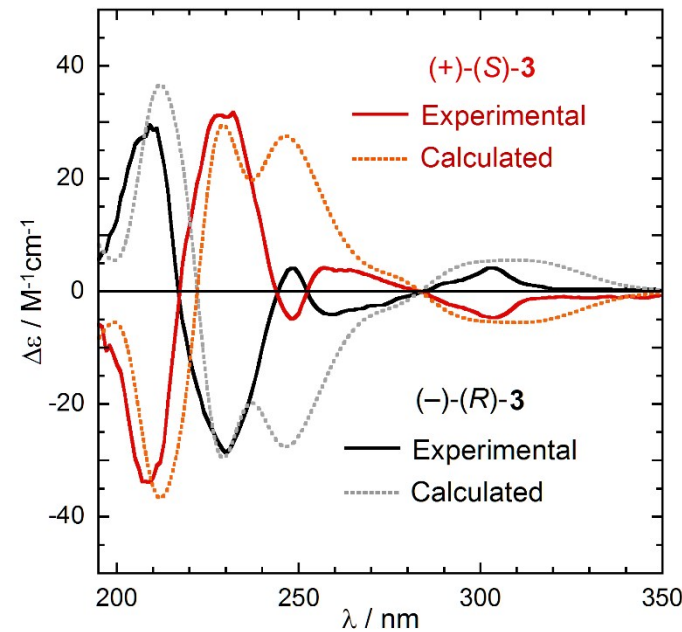


Fig. S4 Torsional energy scans around the biaryl axis computed at B97X-DD/6-31G(d,p) level. Plotted energy relative to compound **2**.

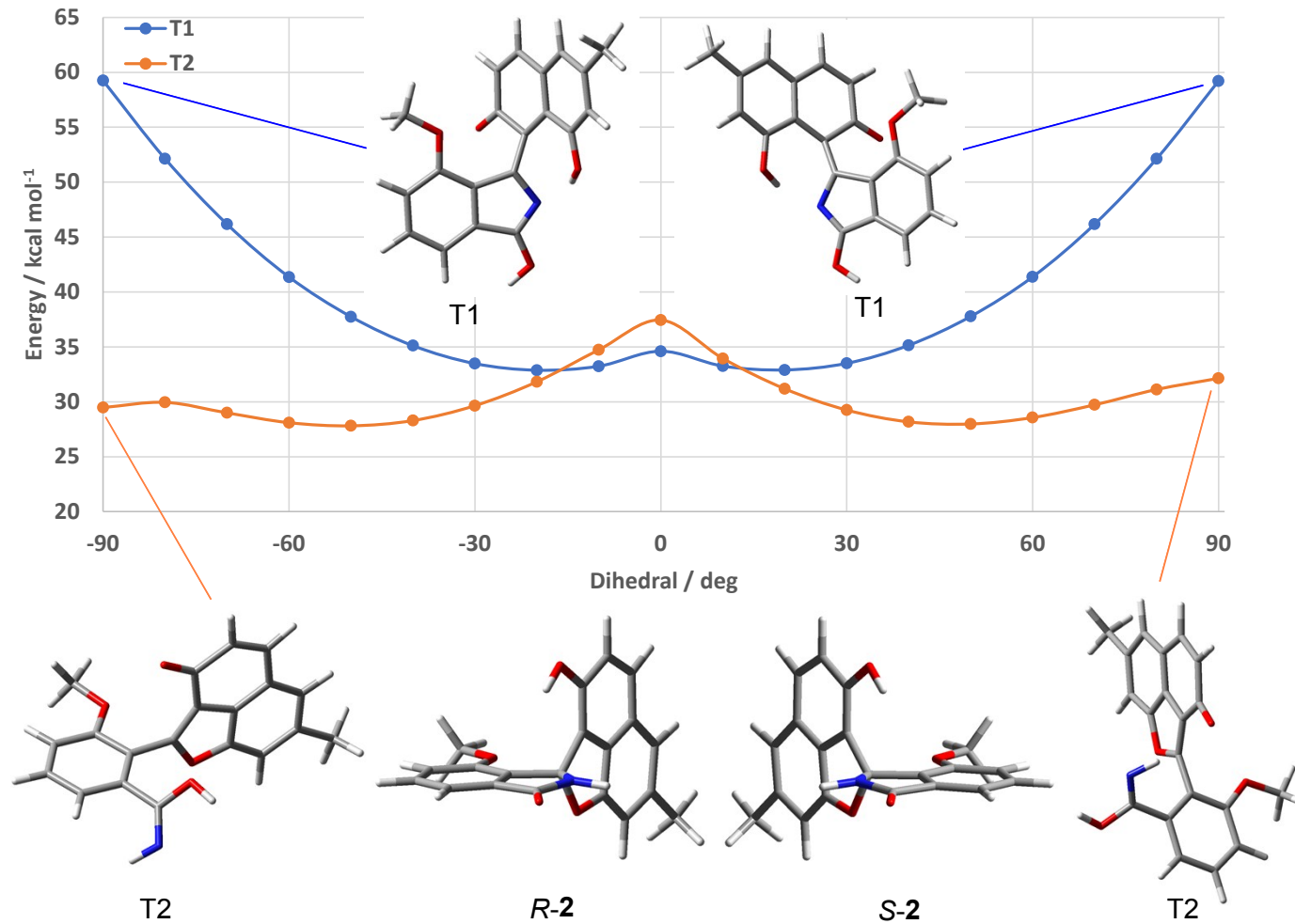


Fig. S5 Torsional energy scans around the biaryl axis computed at B97X-DD/6-31G(d,p) level. Plotted energy relative to compound 3.

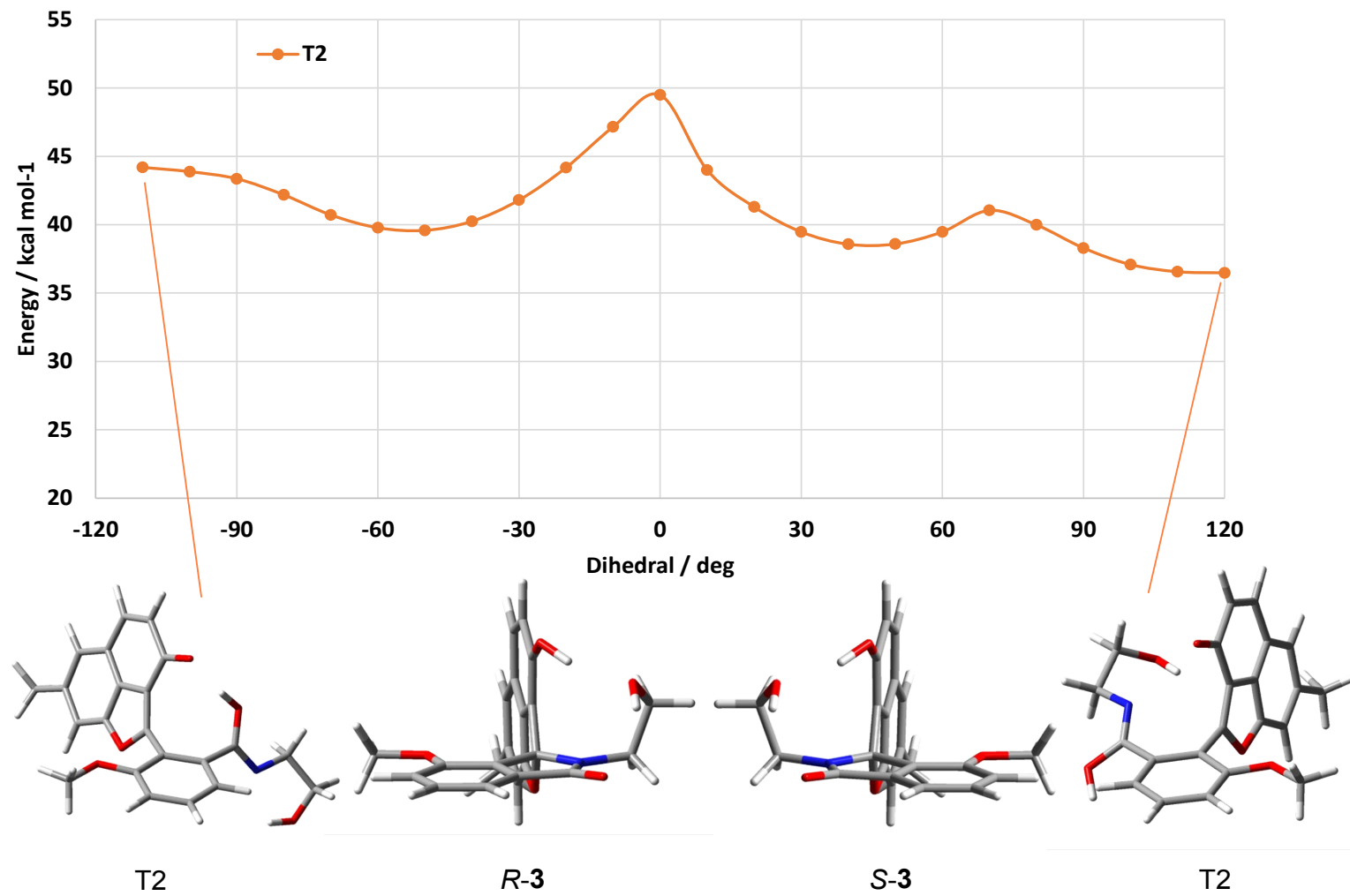


Fig. S6 ^1H NMR spectrum (500 MHz) of (\pm)-pratensilin A (**1**) in $\text{DMSO}-d_6$.

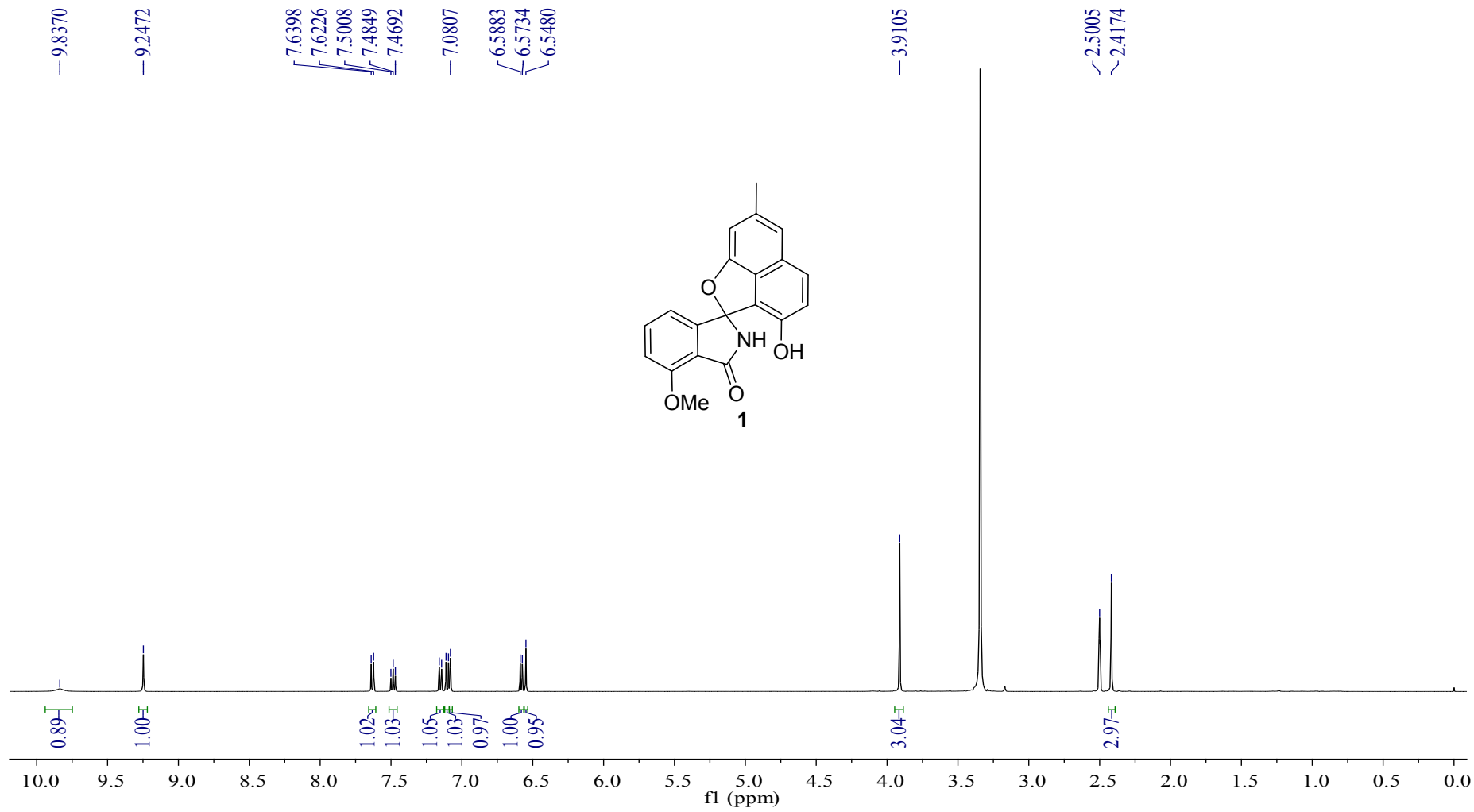


Fig. S7 ^{13}C NMR spectrum (125 MHz) of (\pm)-pratensilin A (**1**) in $\text{DMSO}-d_6$.

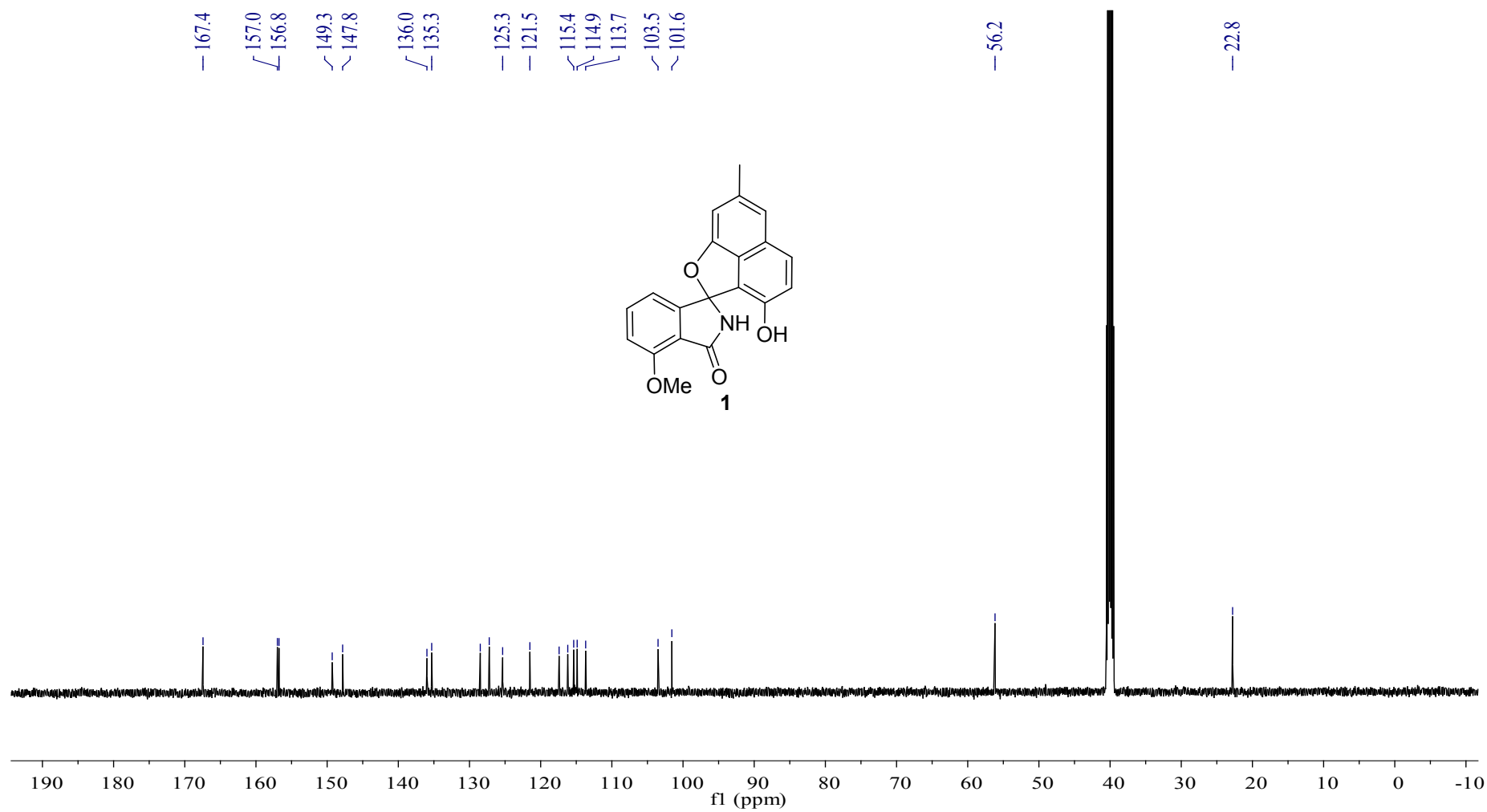


Fig. S8 DEPT-135 spectrum (125 MHz) of (\pm)-pratensilin A (**1**) in DMSO-*d*₆.

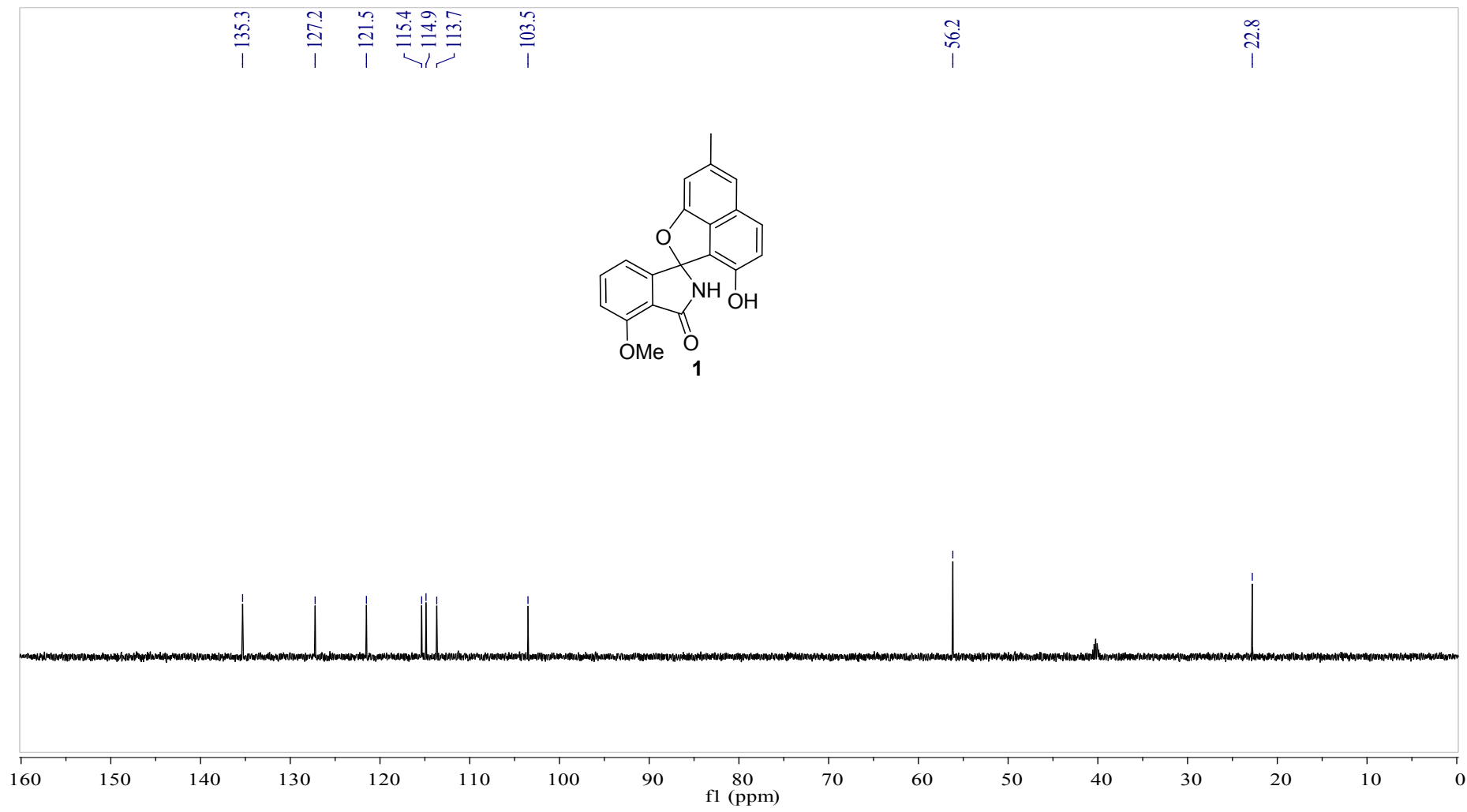


Fig. S9 COSY spectrum (500 MHz) of (\pm)-pratensilin A (**1**) in DMSO-*d*₆.

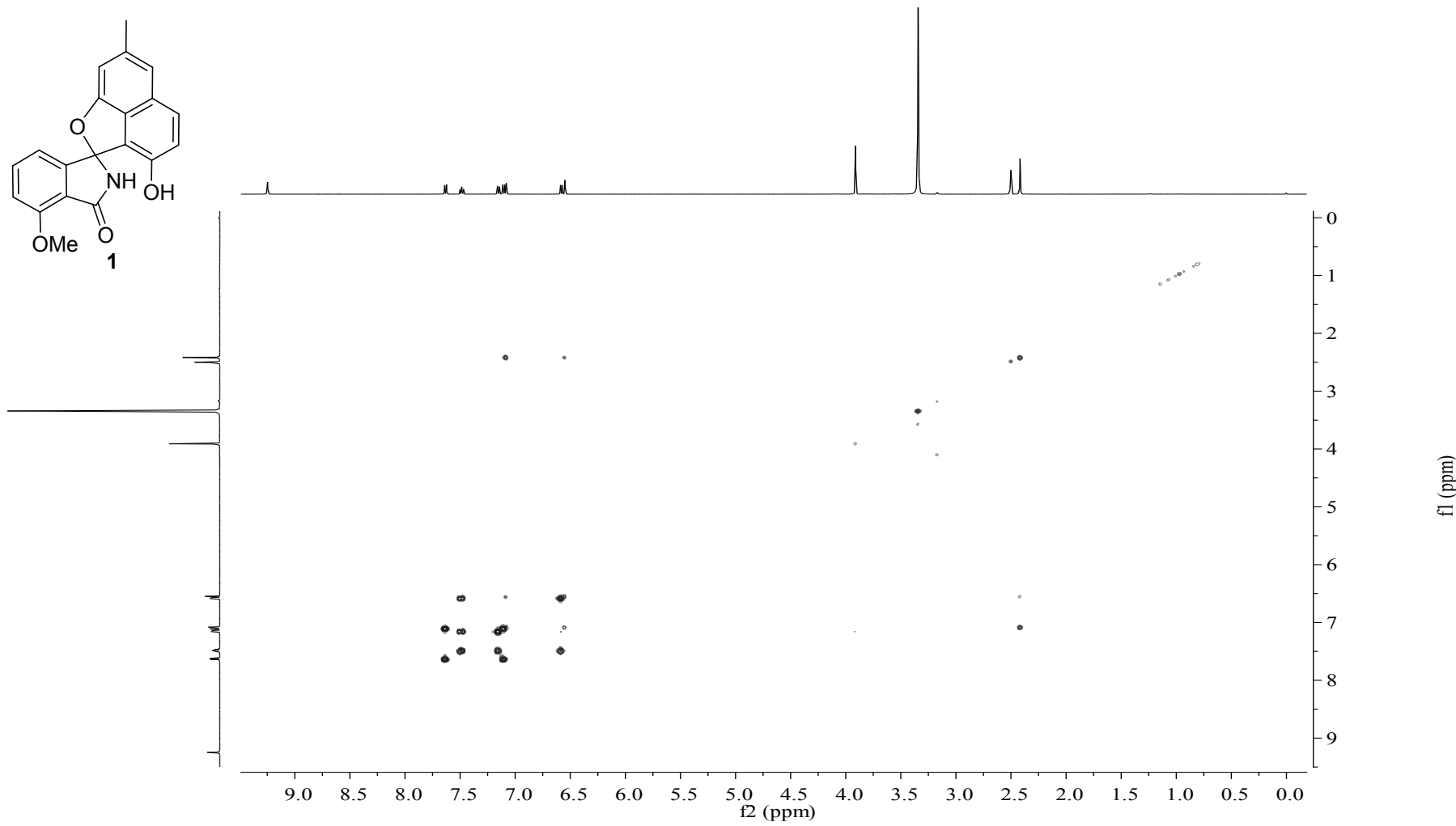


Fig. S10 HSQC spectrum (500 MHz) of (\pm)-pratensilin A (**1**) in DMSO-*d*₆.

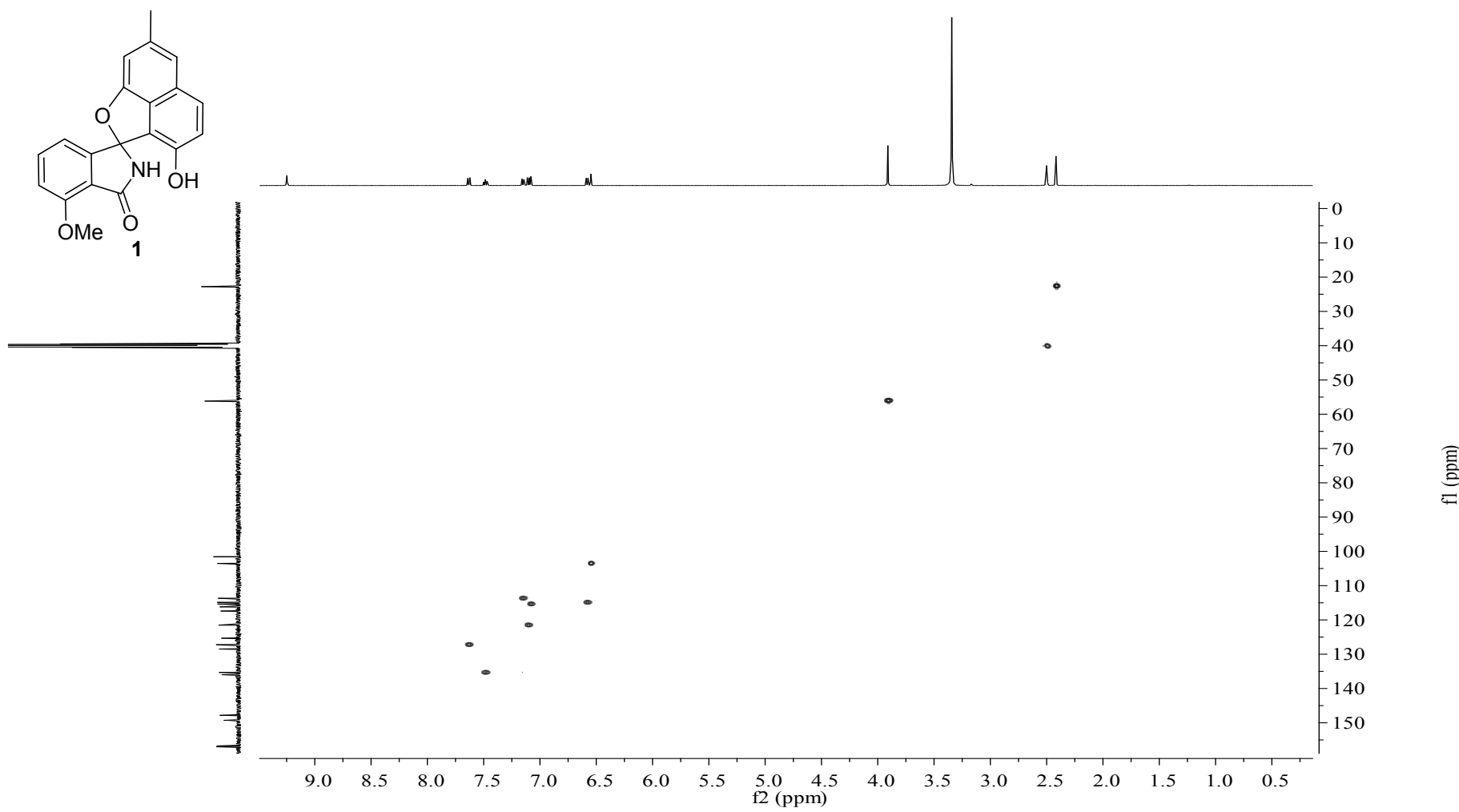


Fig. S11 HMBC spectrum (500 MHz) of (\pm)-pratensilin A (**1**) in DMSO-*d*₆.

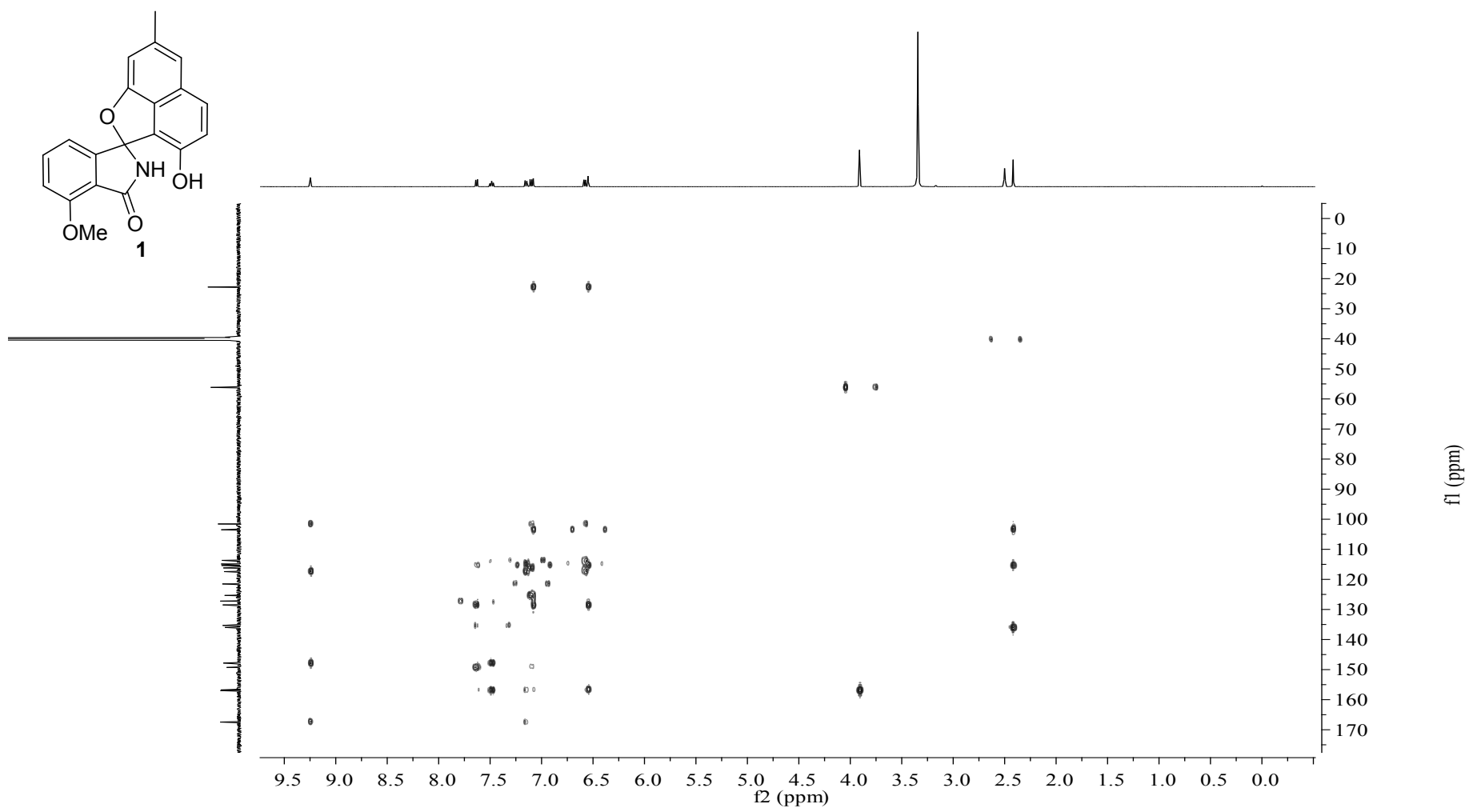


Fig. S12 NOESY spectrum (500 MHz) of (\pm)-pratensilin A (**1**) in DMSO-*d*₆.

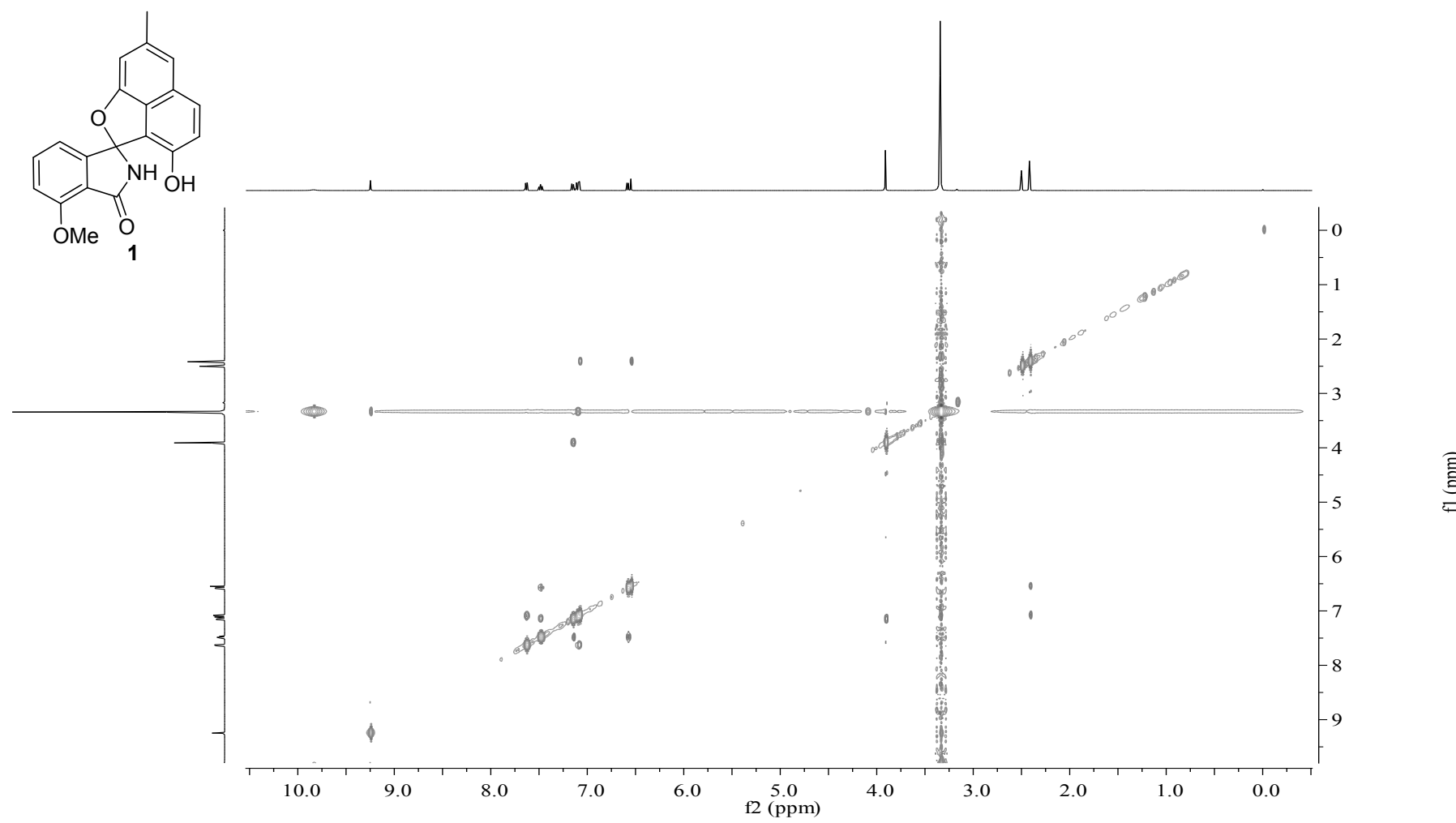


Fig. S13 HRESIMS spectrum of (\pm)-pratensilin A (**1**).

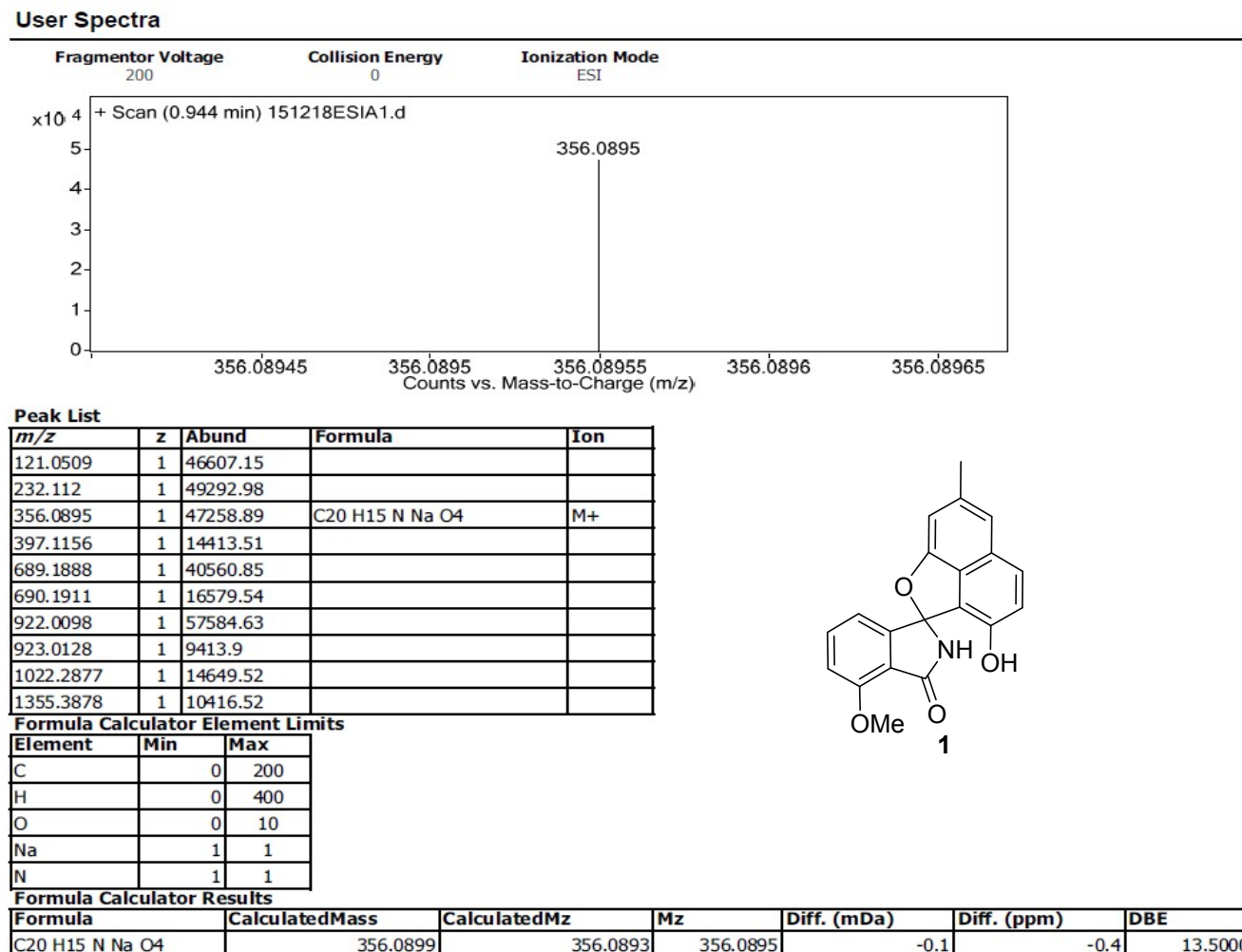


Fig. S14 UV spectrum of (+)-pratensilin A ((+)-**1**).

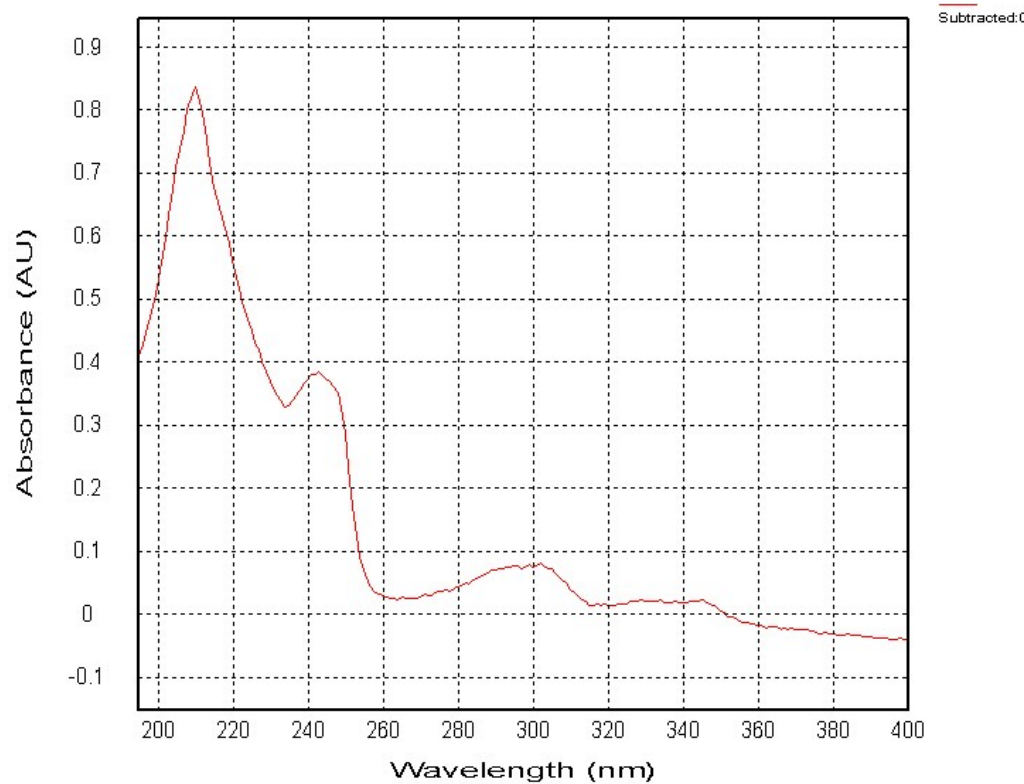


Fig. S15 UV spectrum of (-)-pratensilin A ((-)-1).

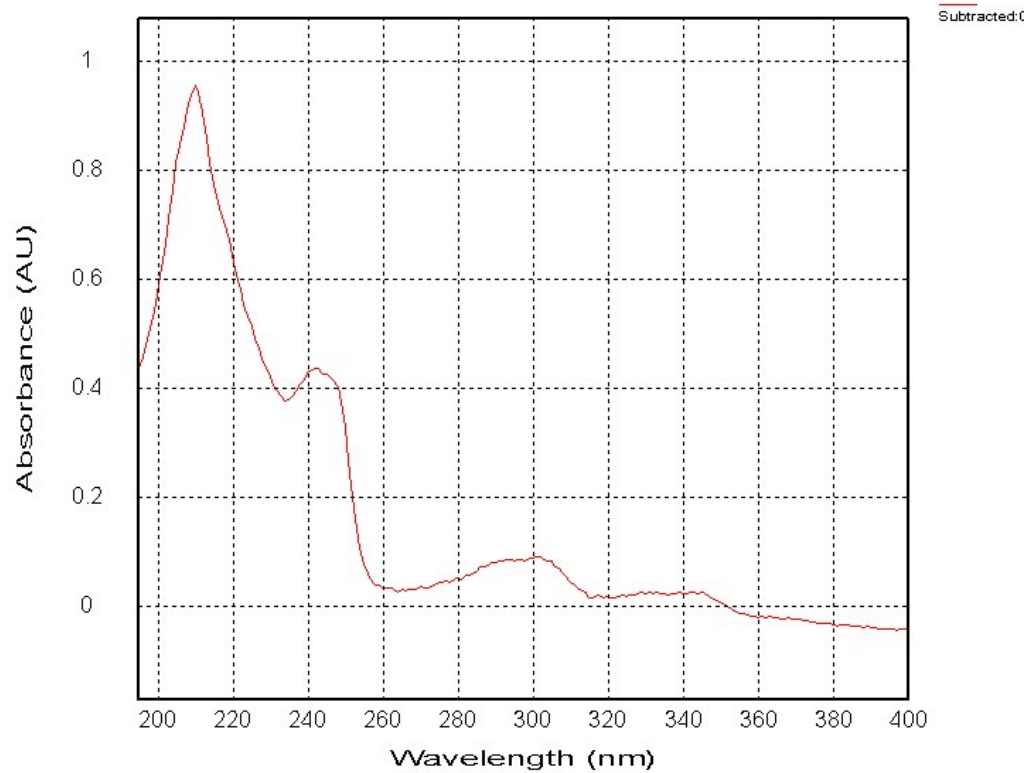


Fig. S16 IR spectrum of (\pm)-pratensilin A (**1**).

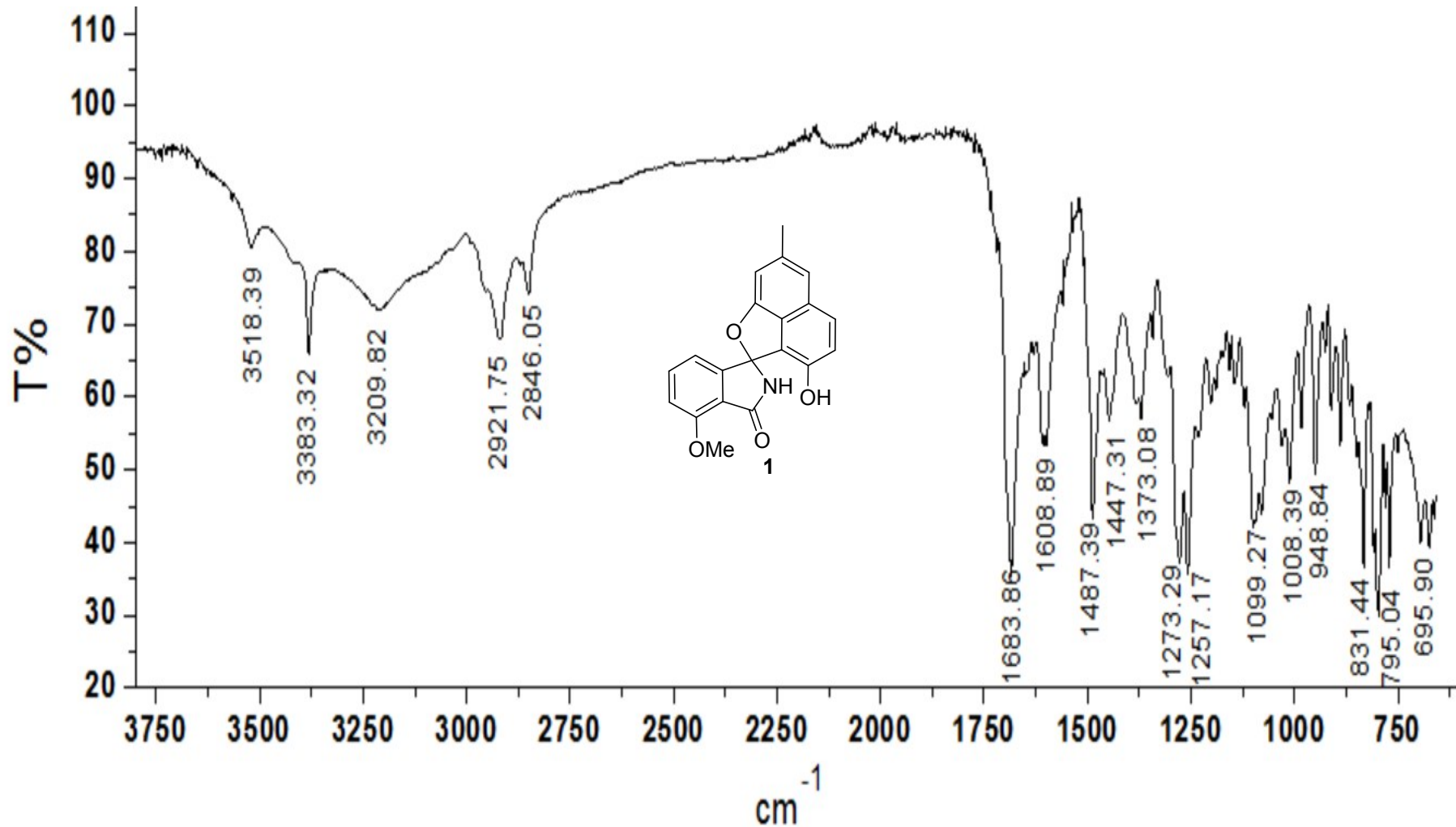


Fig. S17 ^1H NMR spectrum (500 MHz) of (\pm)-pratensilin B (**2**) in $\text{DMSO}-d_6$.

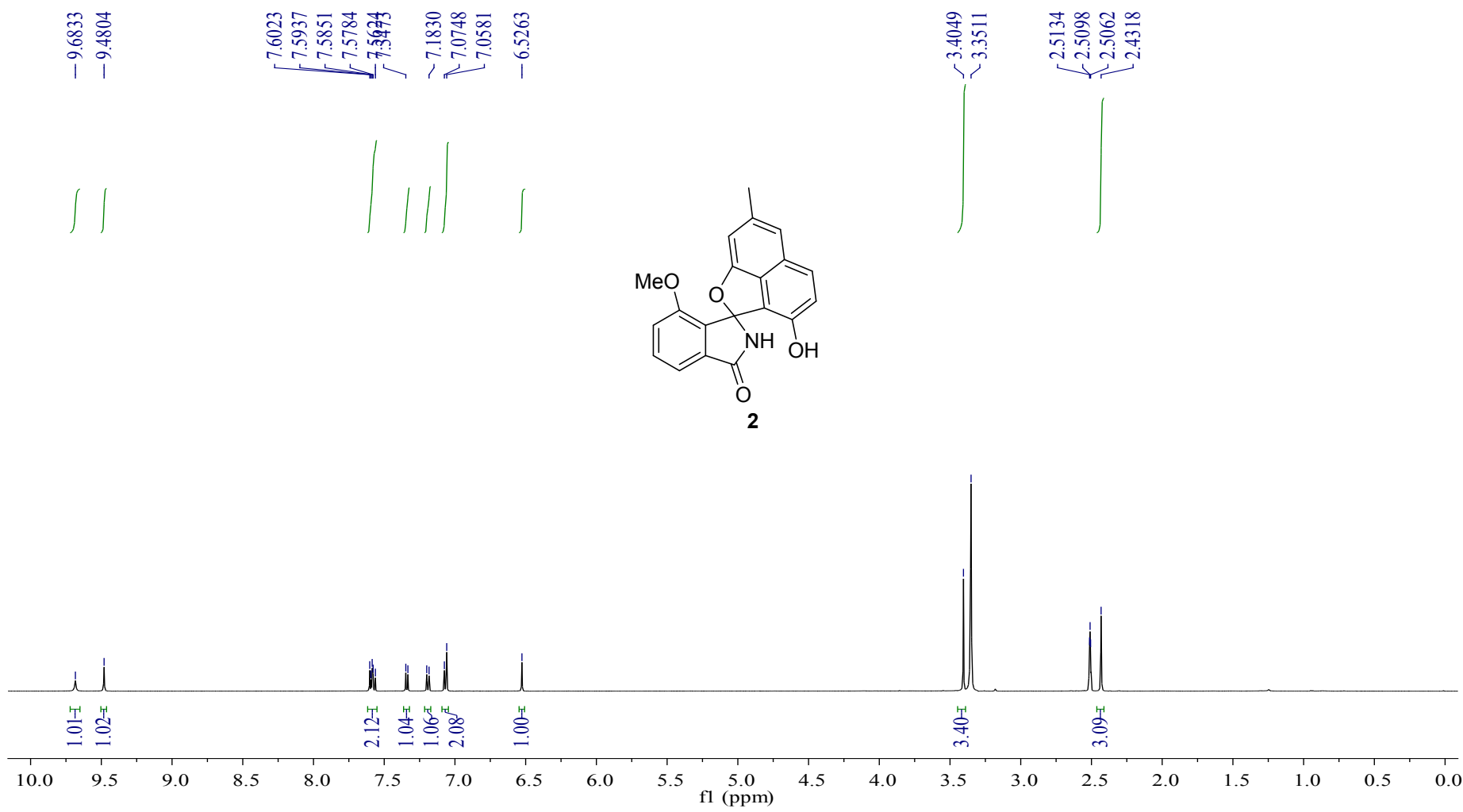


Fig. S18 ^{13}C NMR spectrum (125 MHz) of (\pm)-pratensilin B (**2**) in $\text{DMSO}-d_6$.

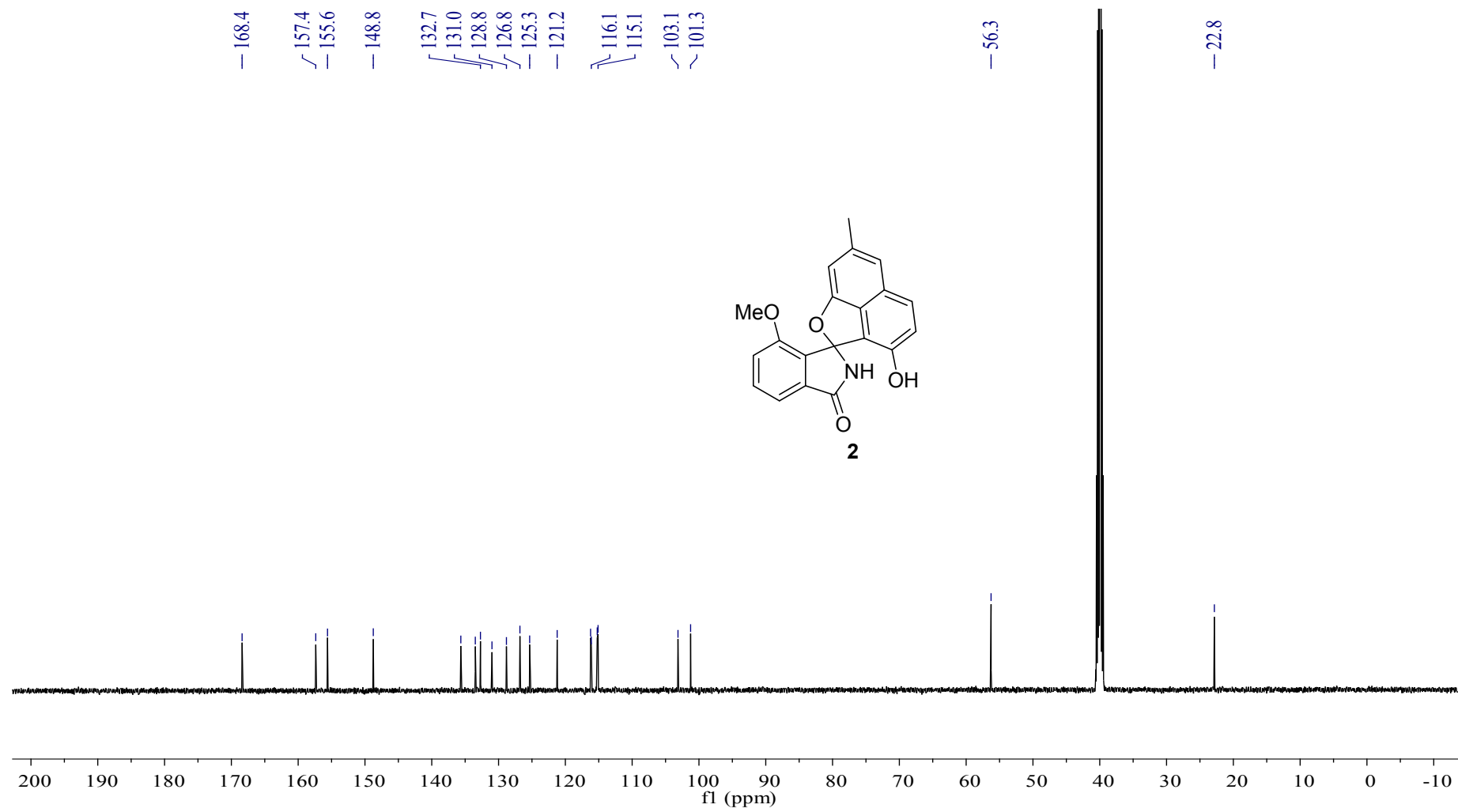


Fig. S19 DEPT-135 spectrum (125 MHz) of (\pm)-pratensilin B (**2**) in DMSO-*d*₆.

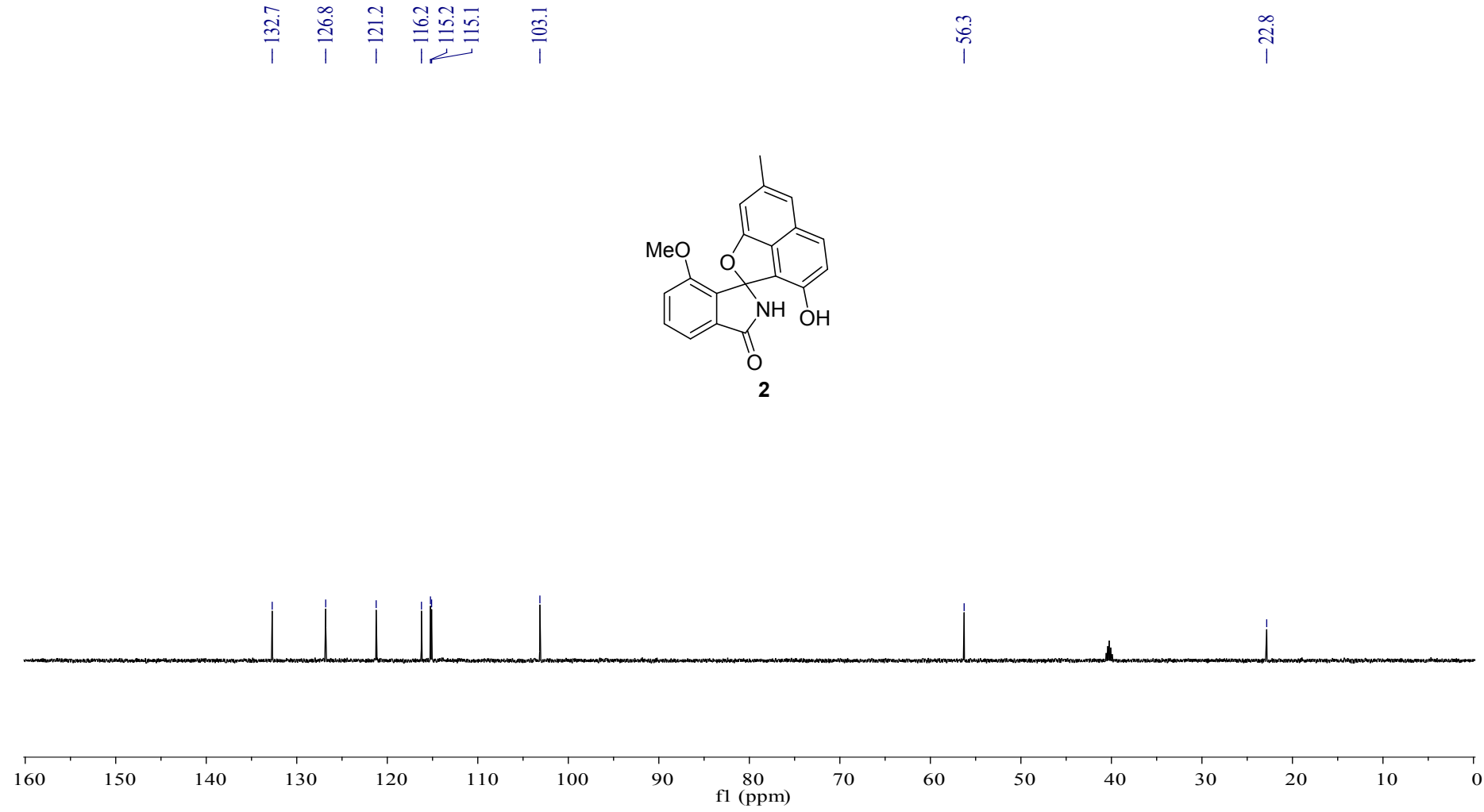


Fig. S20 COSY spectrum (500 MHz) of (\pm)-pratensilin B (**2**) in DMSO-*d*₆.

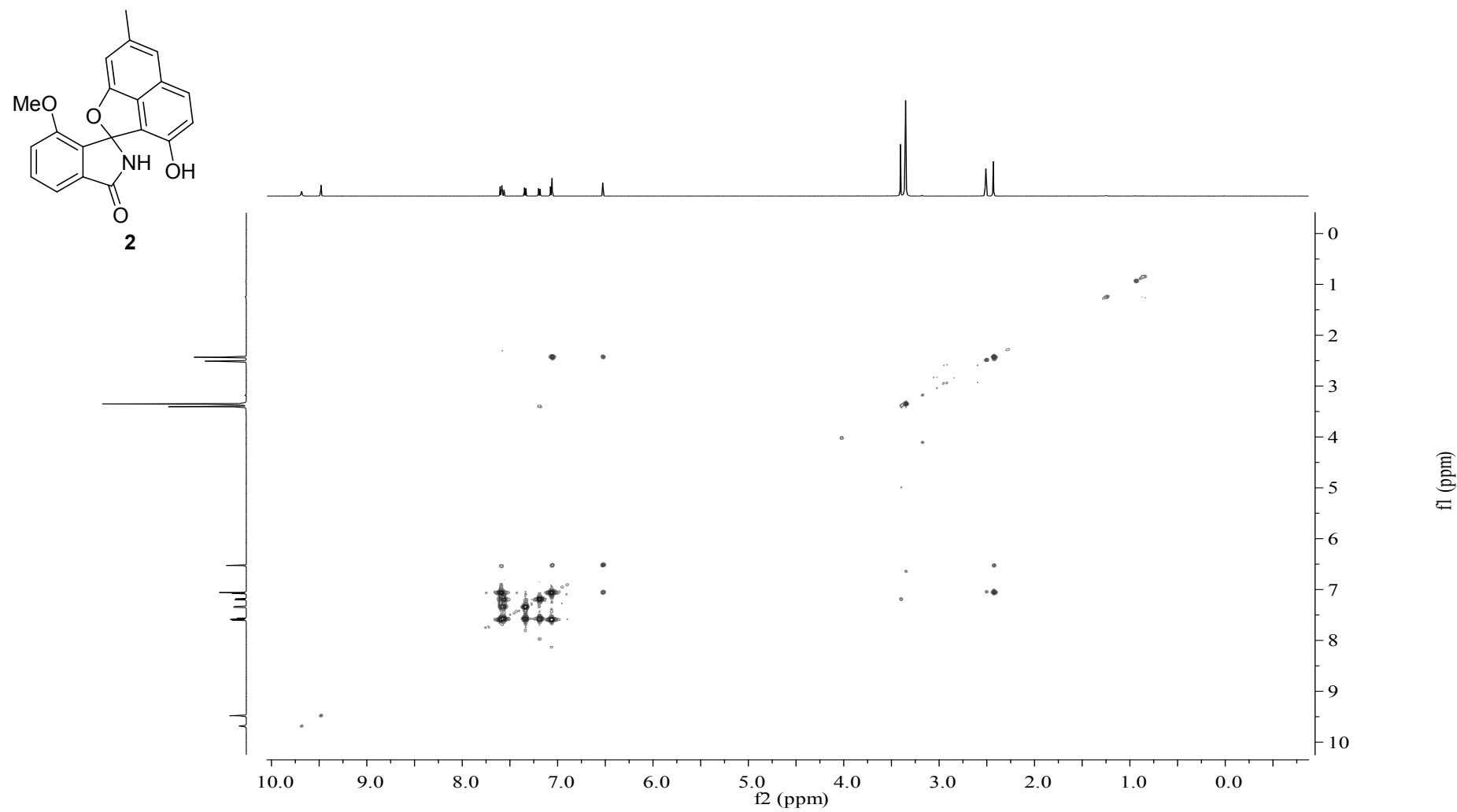


Fig. S21 HSQC spectrum (500 MHz) of (\pm)-pratensilin B (**2**) in DMSO-*d*₆.

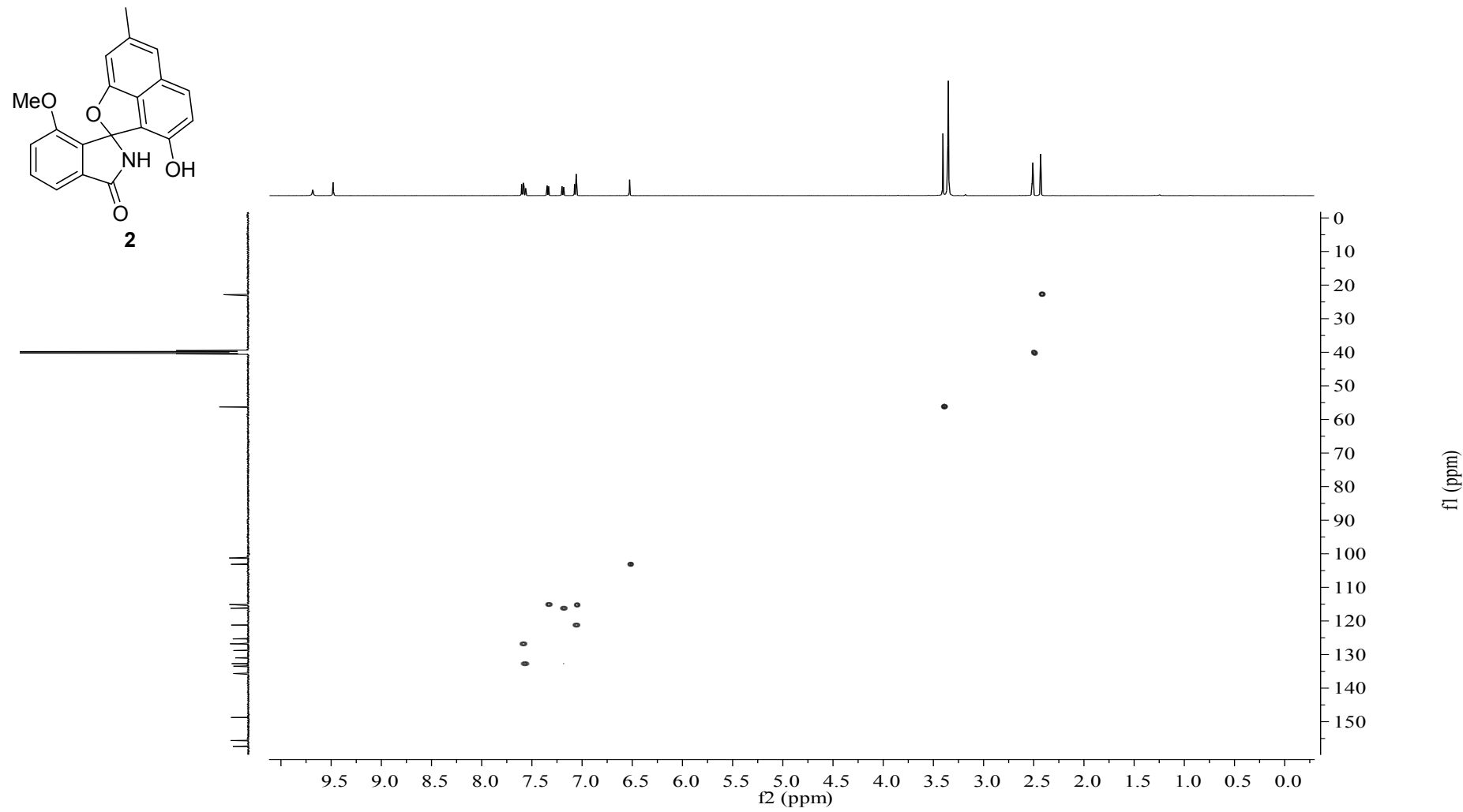


Fig. S22 HMBC spectrum (500 MHz) of (\pm)-pratensilin B (**2**) in DMSO-*d*₆.

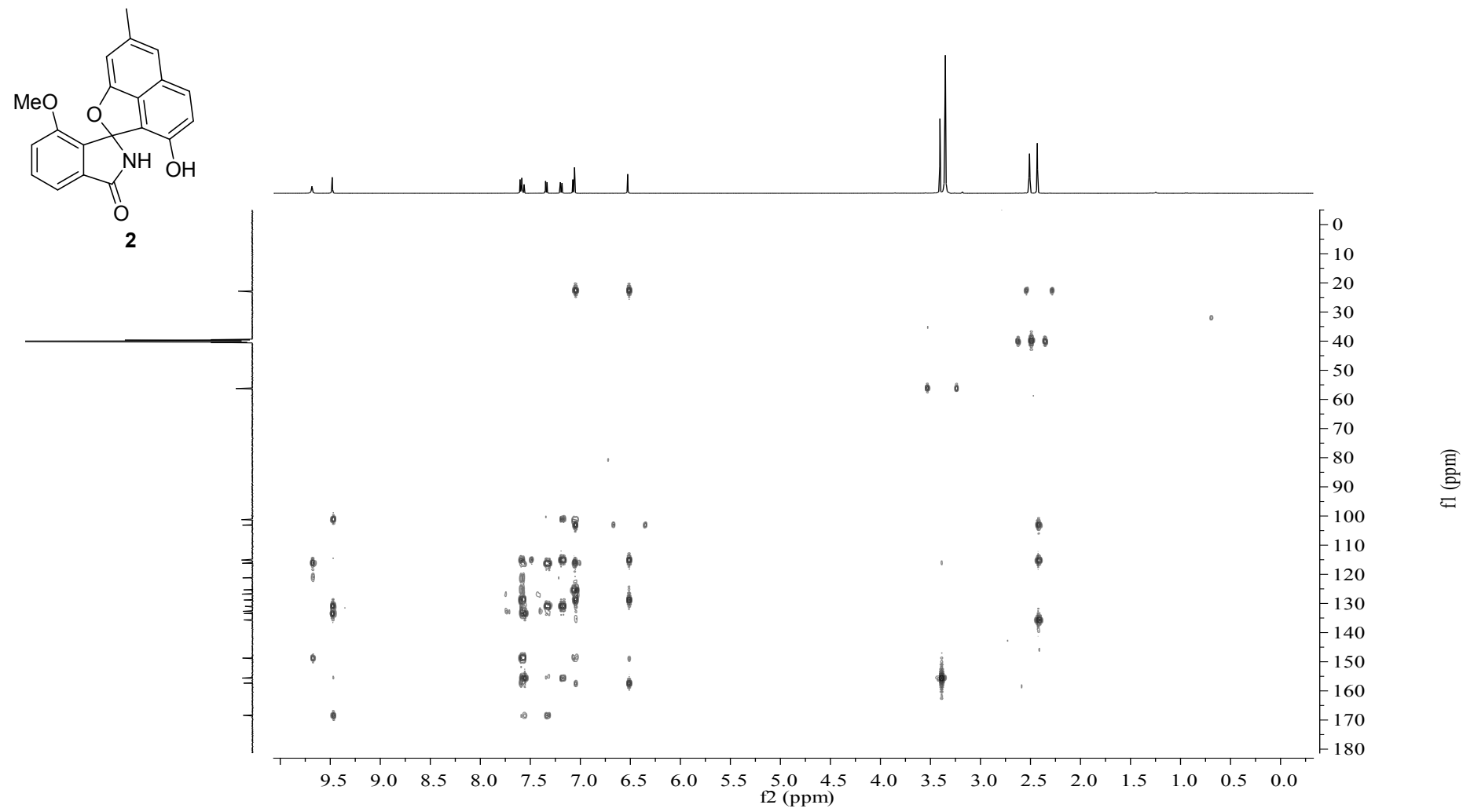


Fig. S23 NOESY spectrum (500 MHz) of (\pm)-pratensilin B (**2**) in DMSO-*d*₆.

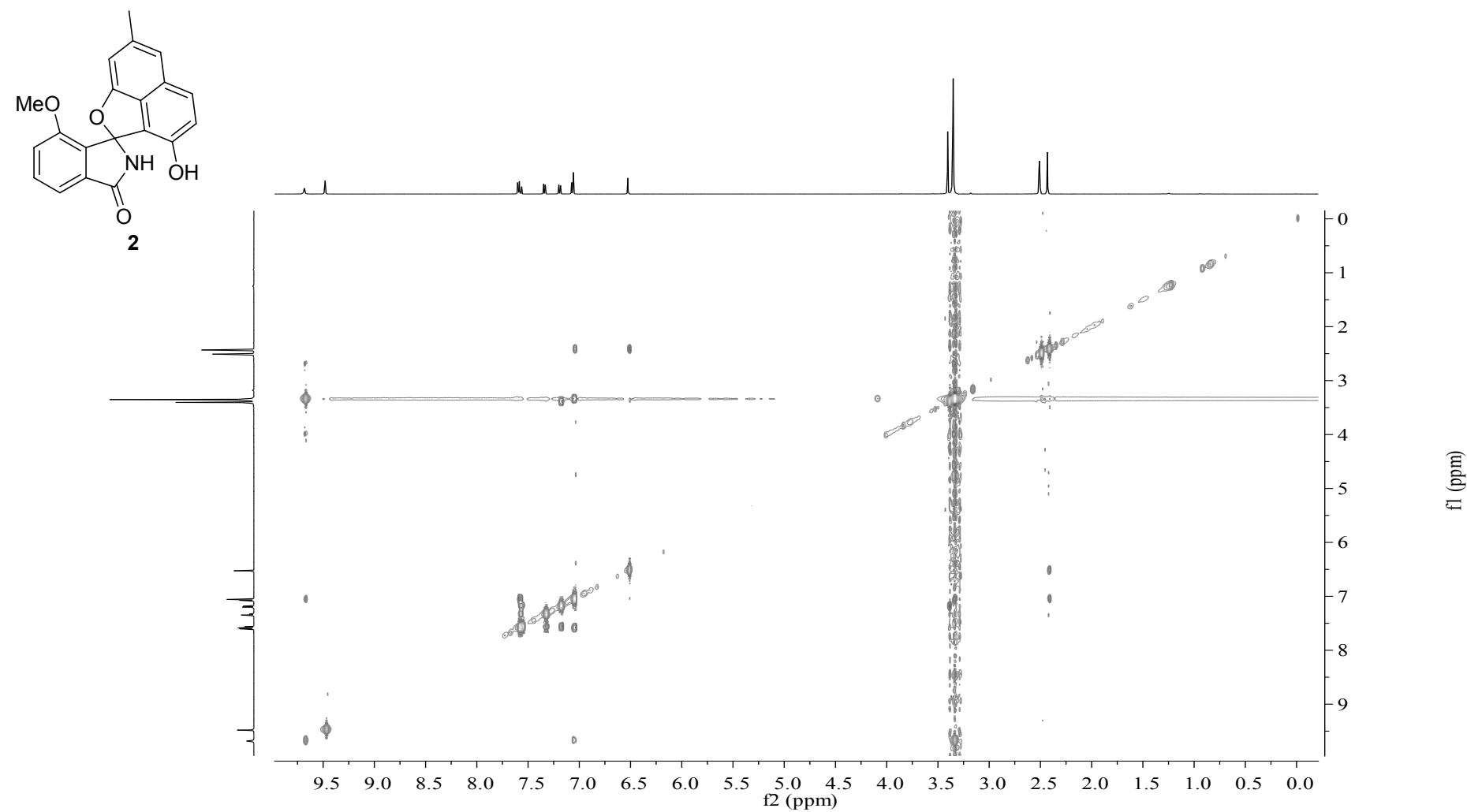


Fig. S24 HRESIMS spectrum of (\pm)-pratensilin B (**2**).

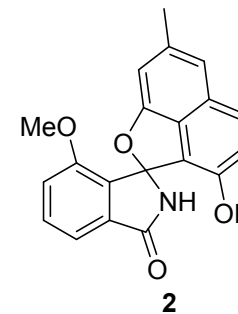
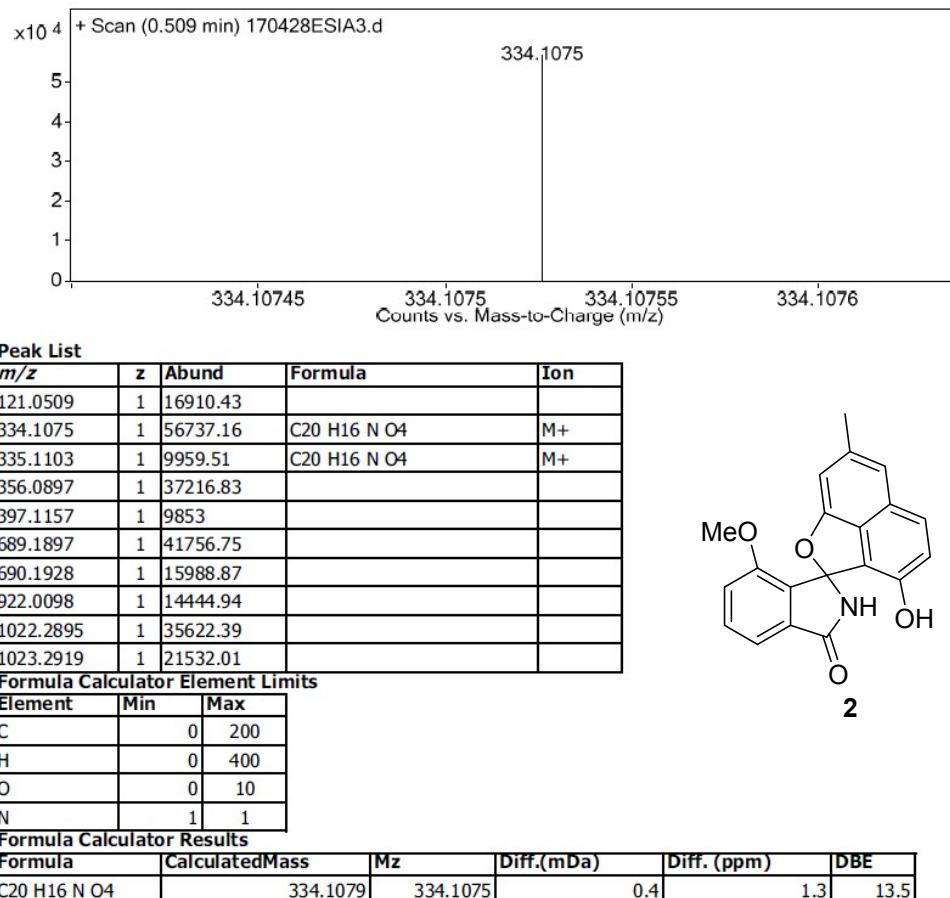


Fig. S25 UV spectrum of (+)-pratensilin B ((+)-2).

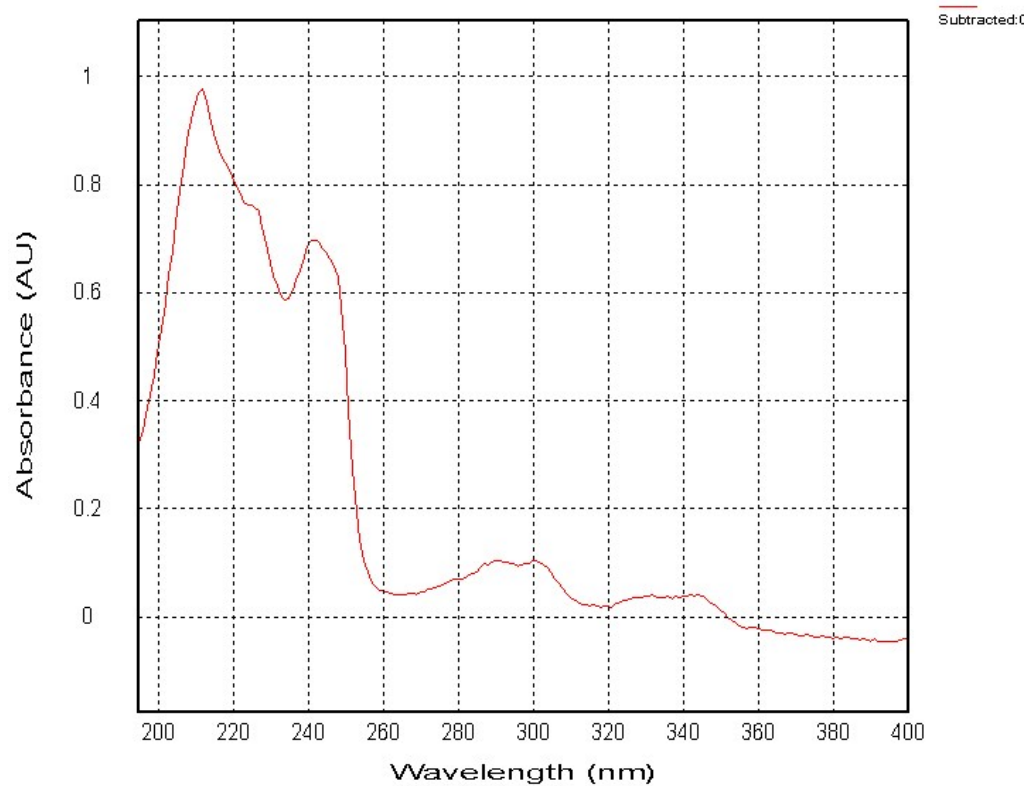


Fig. S26 UV spectrum of (-)-pratensilin B ((-)-2).

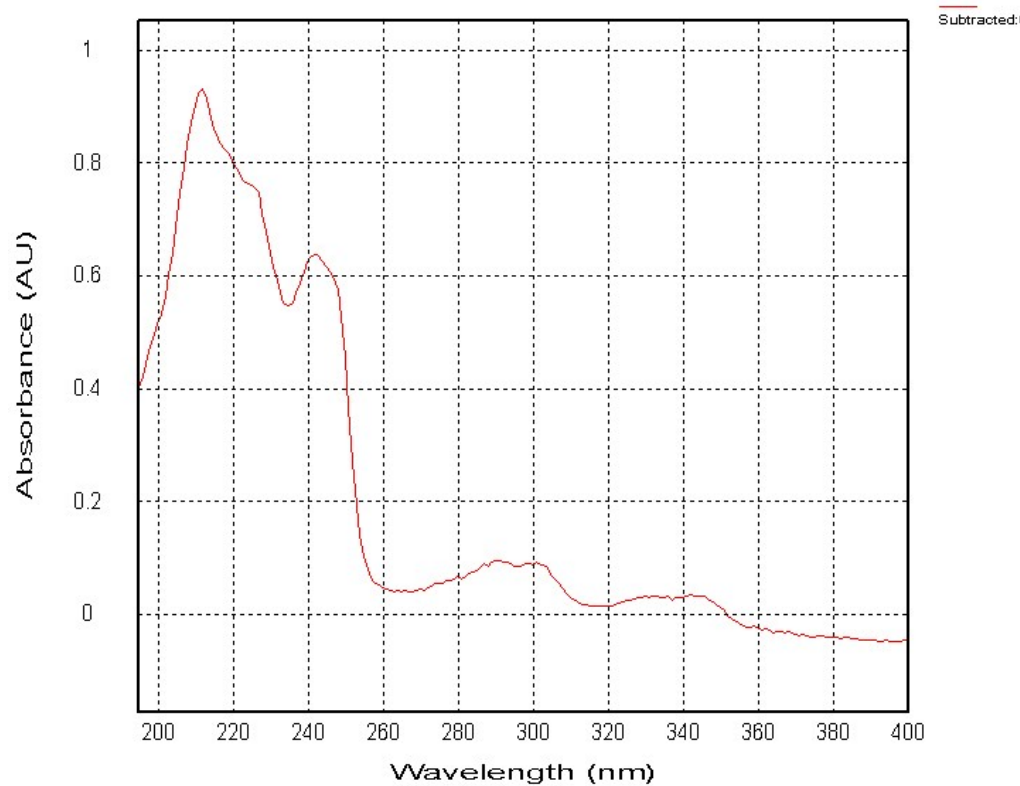


Fig. S27 IR spectrum of (\pm)-pratensilin B (**2**).

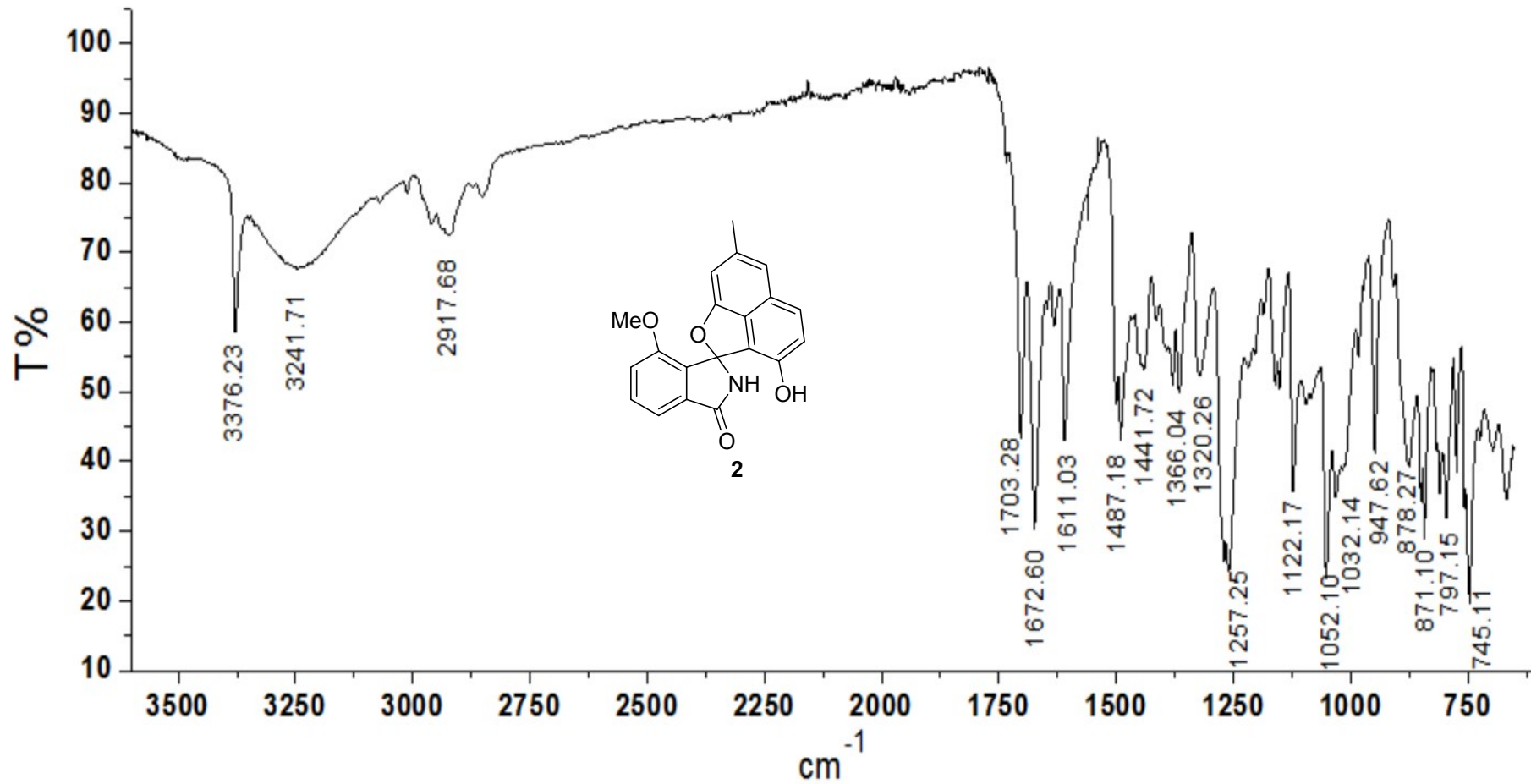


Fig. S28 ^1H NMR spectrum (500 MHz) of (\pm)-pratensilin C (**3**) in $\text{DMSO}-d_6$.

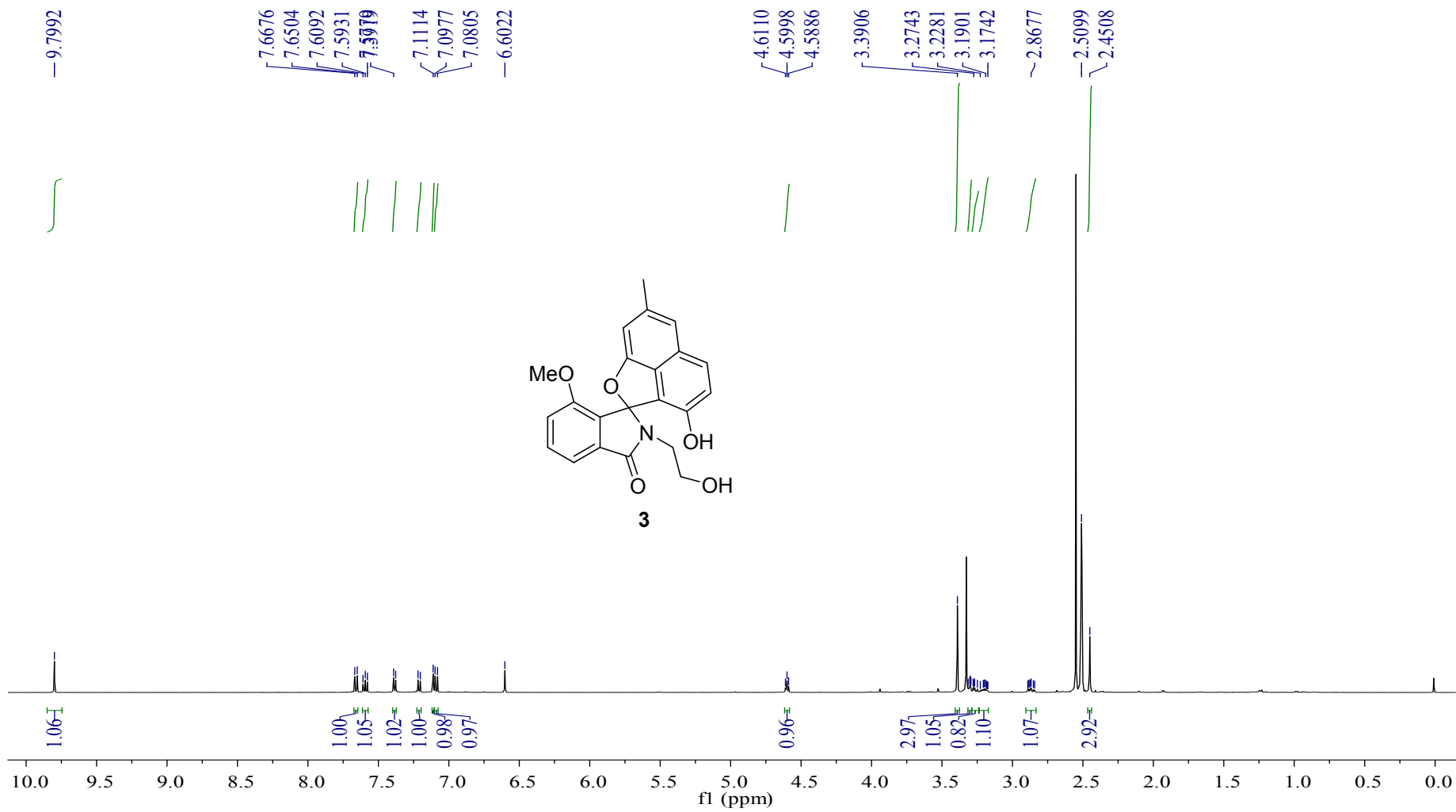


Fig. S29 ^{13}C NMR spectrum (125 MHz) of (\pm)-pratensilin C (**3**) in $\text{DMSO}-d_6$.

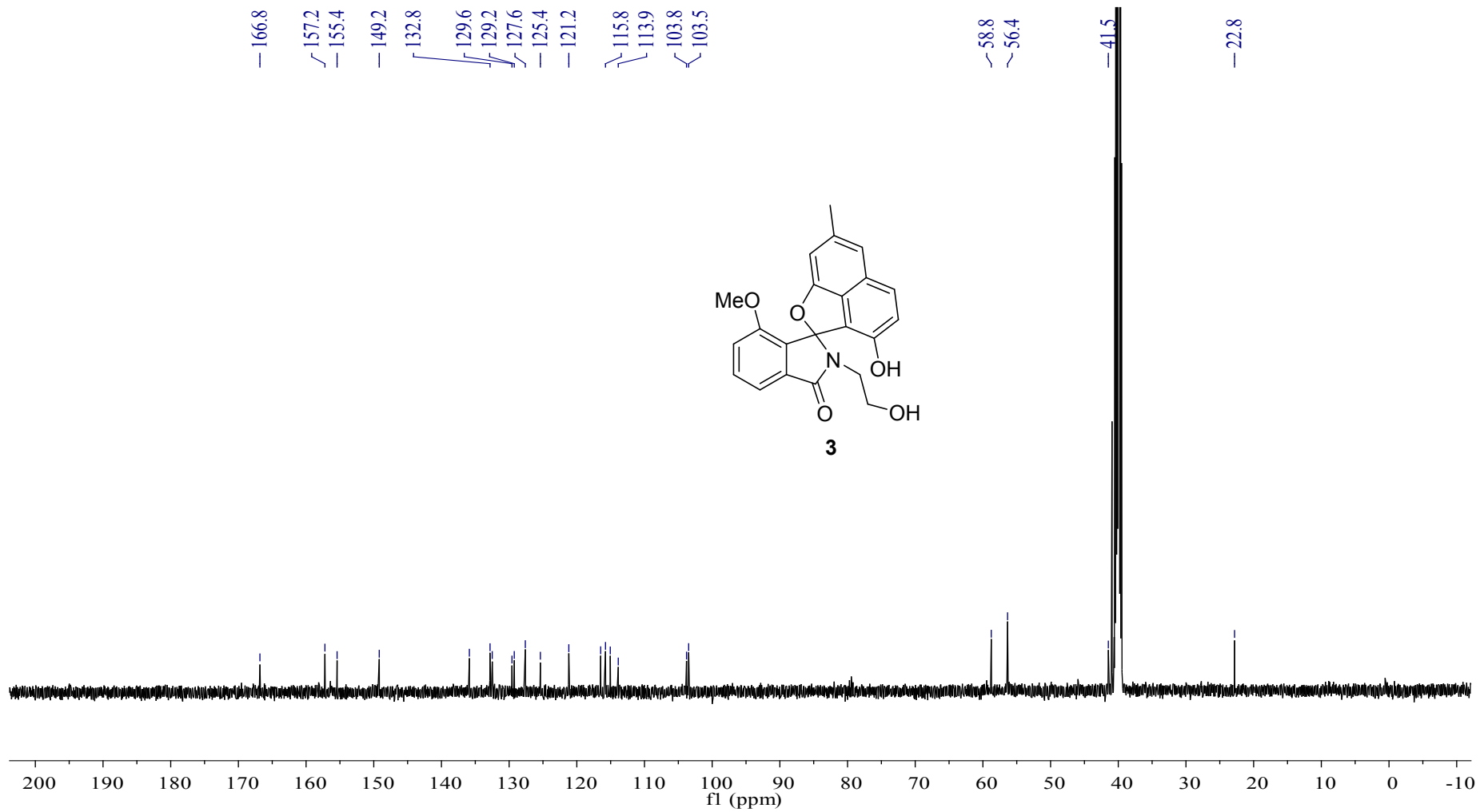


Fig. S30 DEPT-135 spectrum (125 MHz) of (\pm)-pratensilin C (**3**) in DMSO-*d*₆.

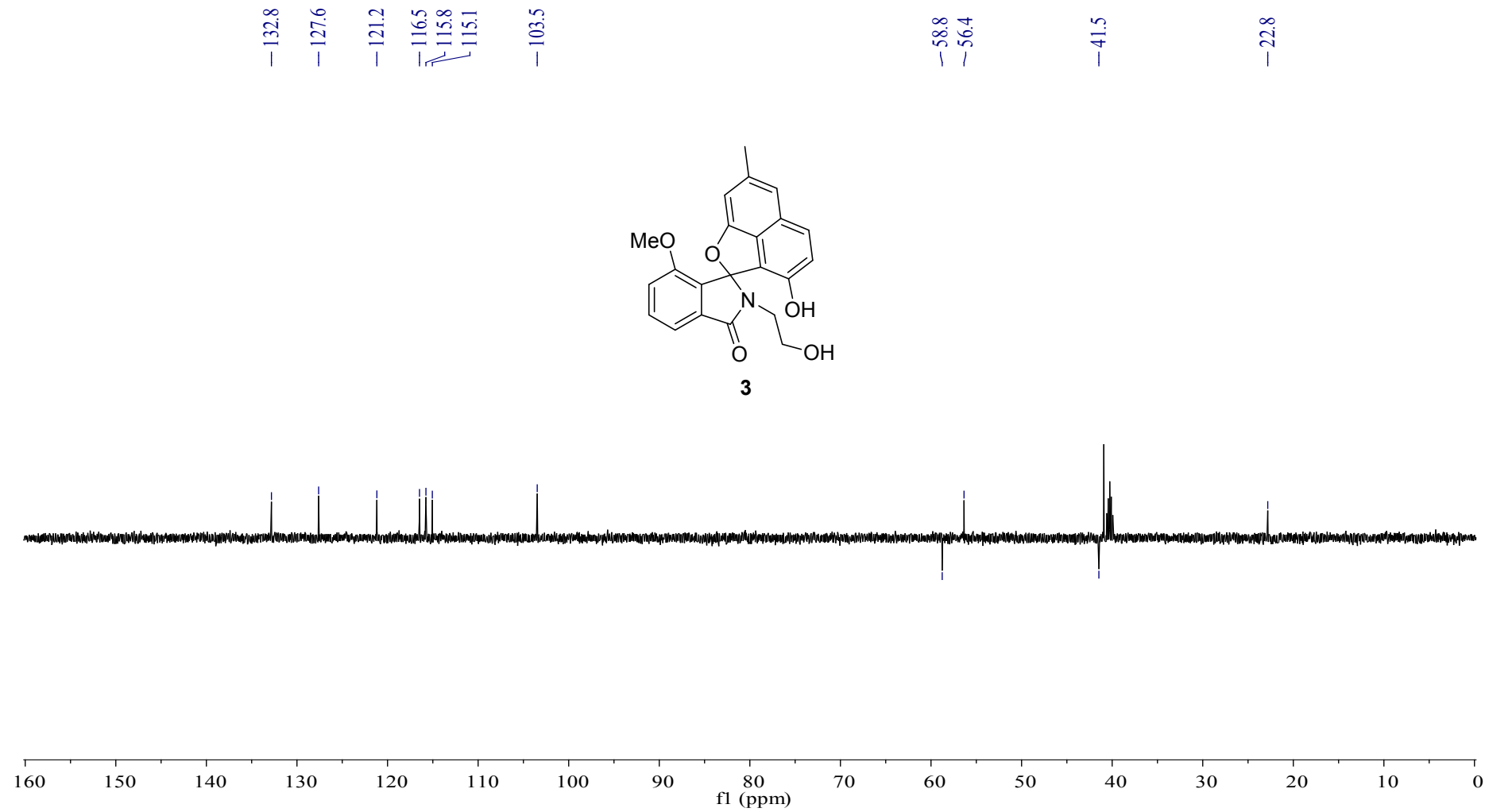


Fig. S31 COSY spectrum (500 MHz) of (\pm)-pratensilin C (**3**) in $\text{DMSO}-d_6$.

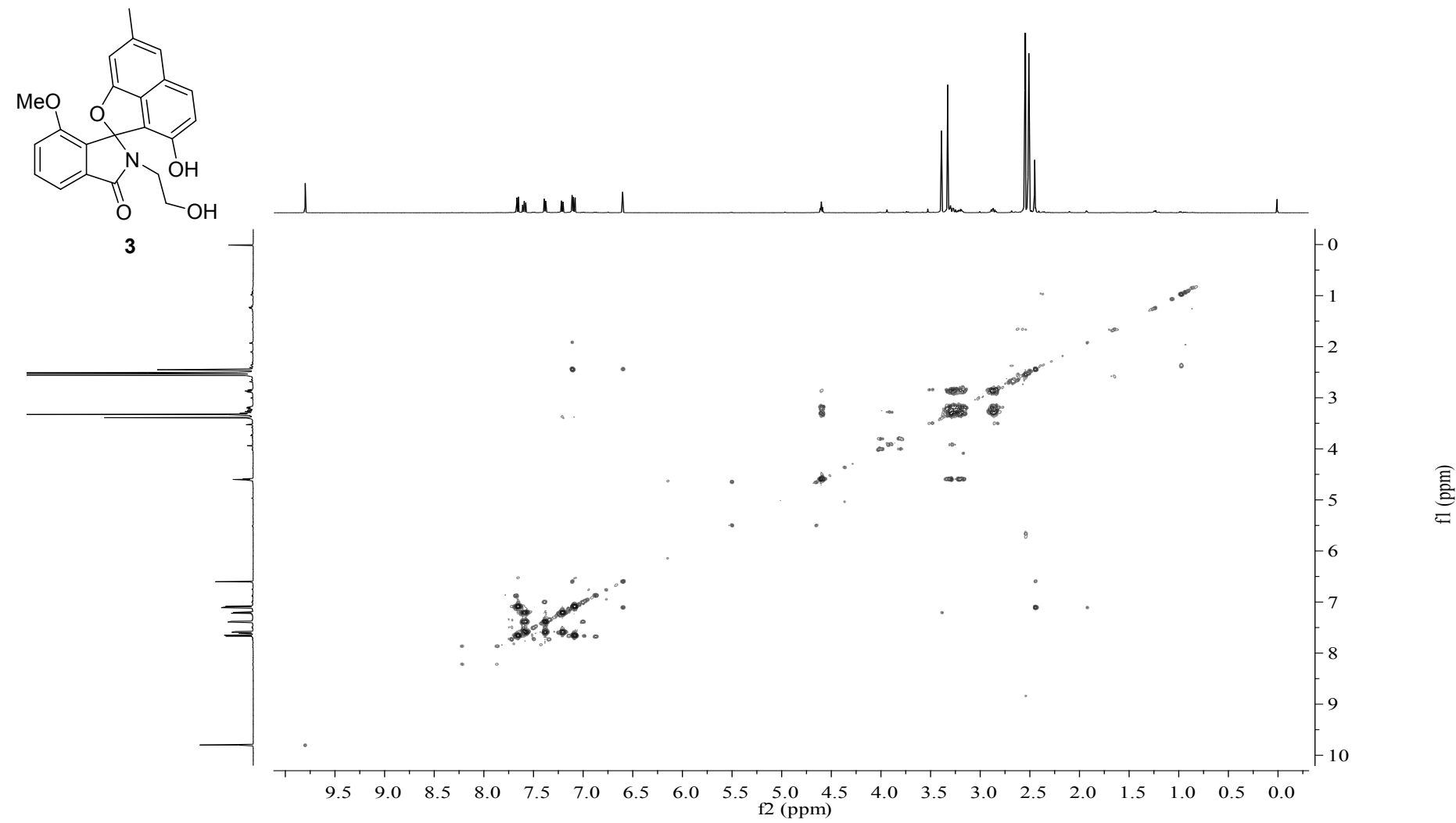


Fig. S32 HSQC spectrum (500 MHz) of (\pm)-pratensilin C (**3**) in DMSO-*d*₆.

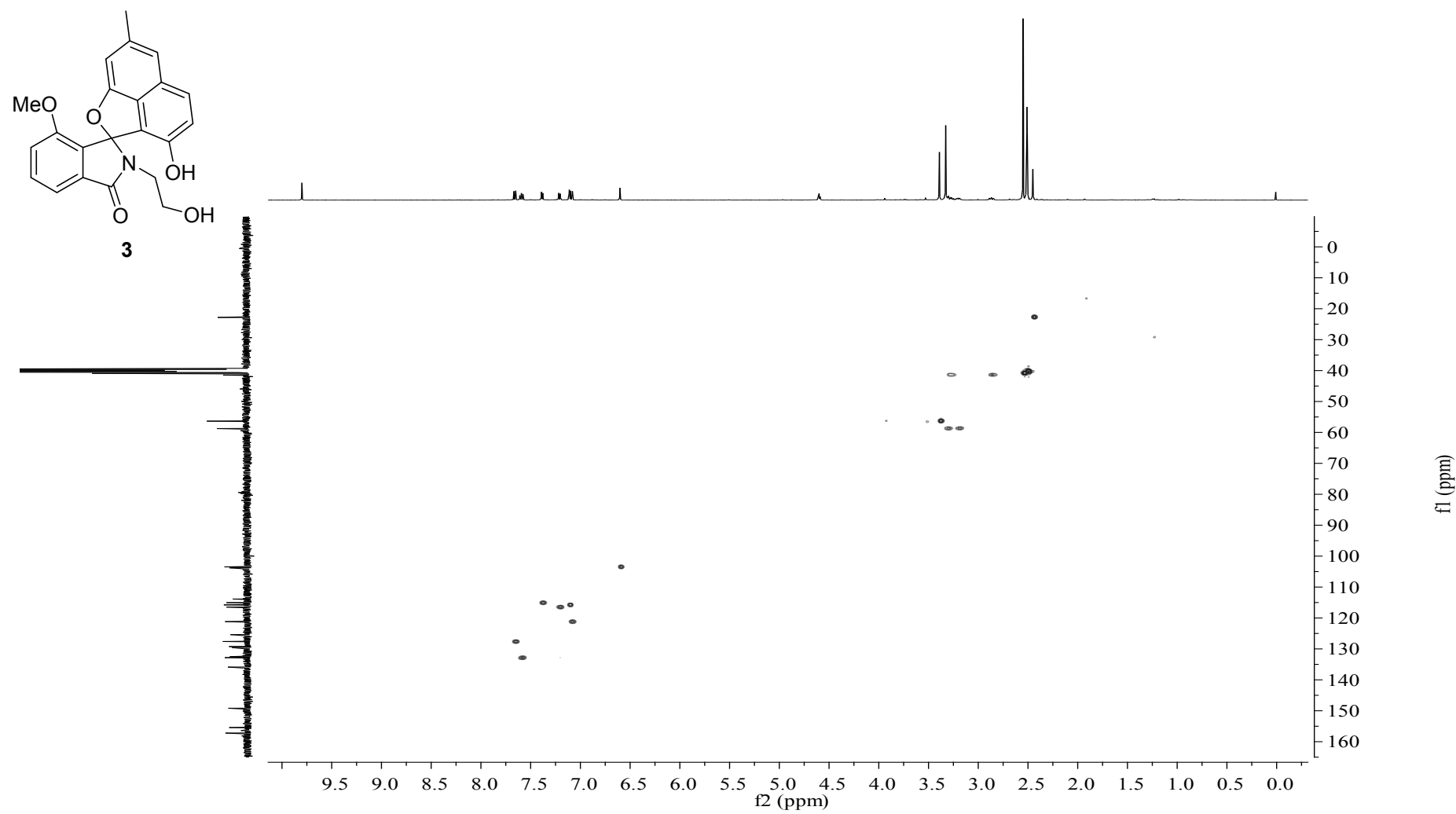


Fig. S33 HMBC spectrum (500 MHz) of (\pm)-pratensilin C (**3**) in DMSO-*d*₆.

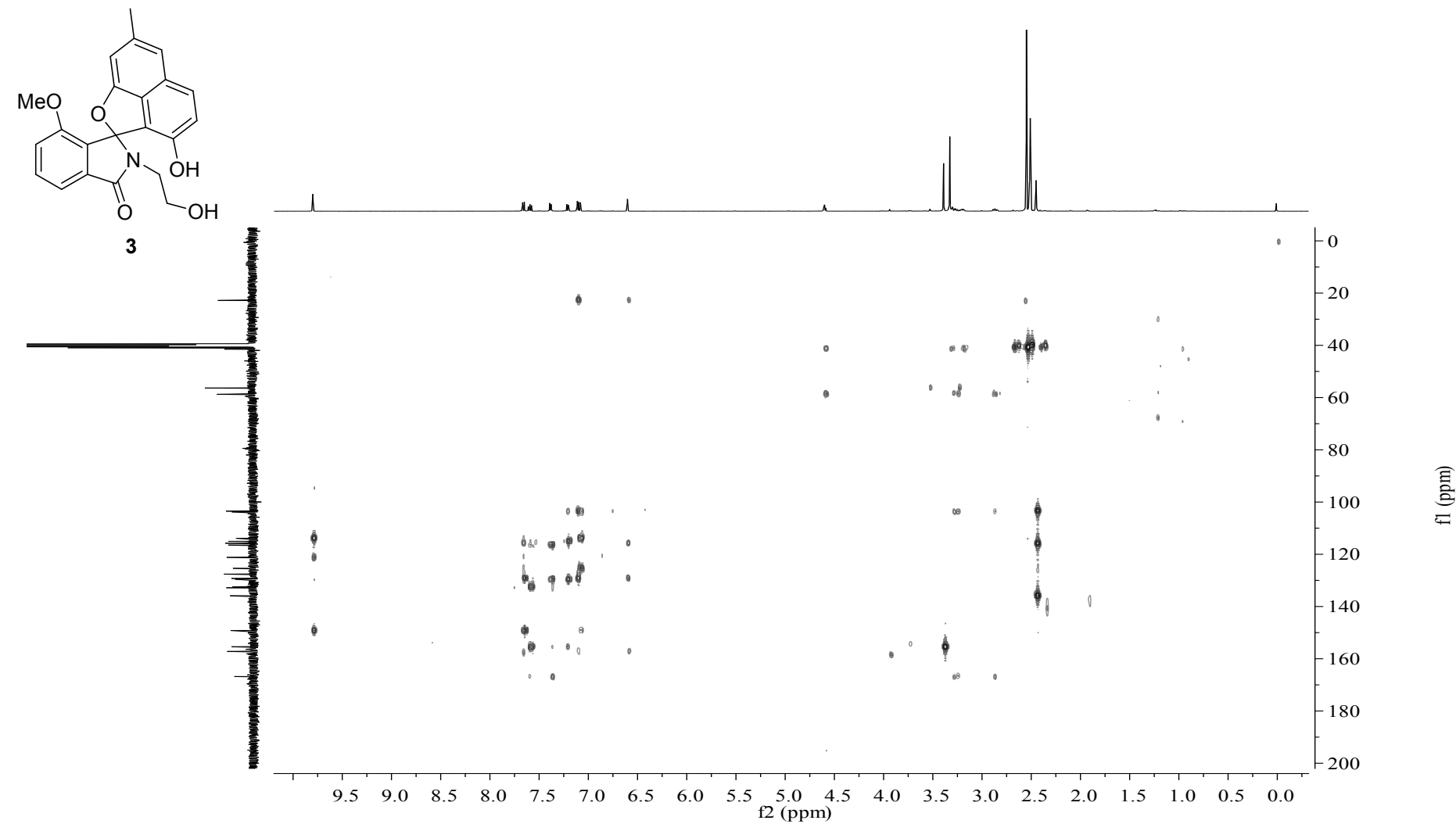


Fig. S34 NOESY spectrum (500 MHz) of (\pm)-pratensilin C (**3**) in DMSO-*d*₆.

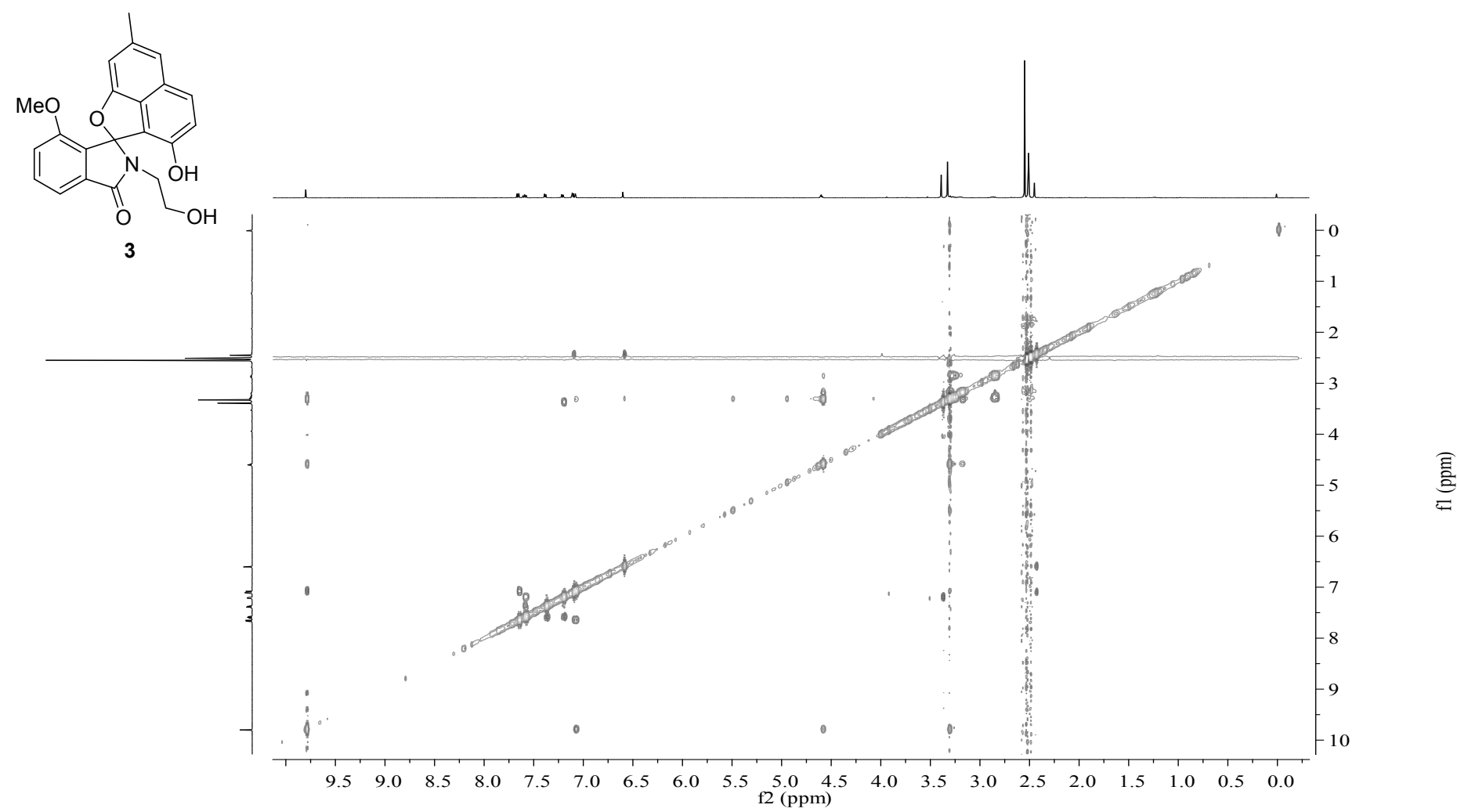


Fig. S35 HRESIMS spectrum of (\pm)-pratensilin C (**3**).

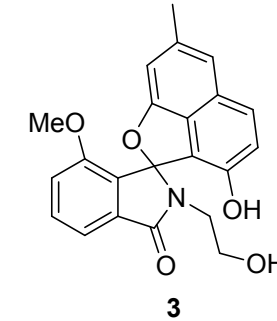
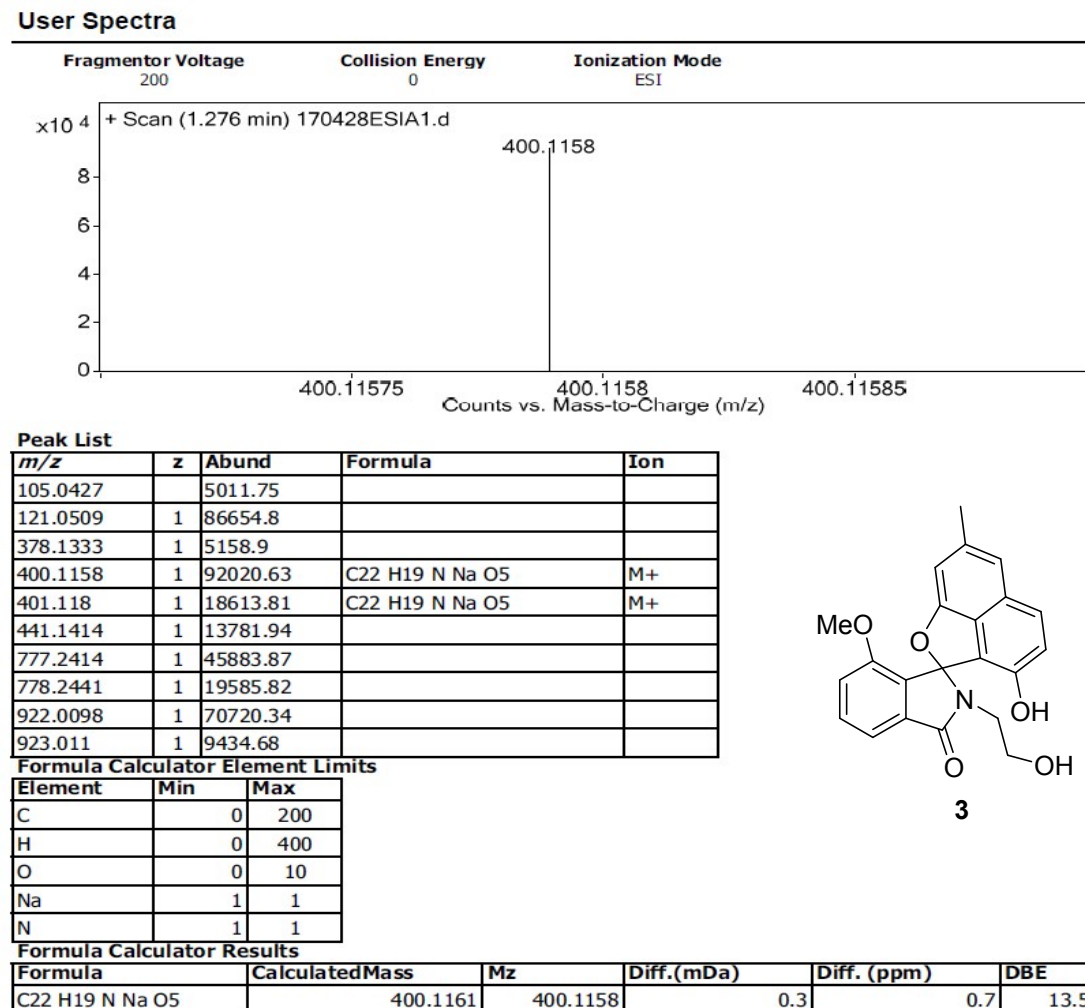


Fig. S36 UV spectrum of (+)-pratensilin C ((+)-3).

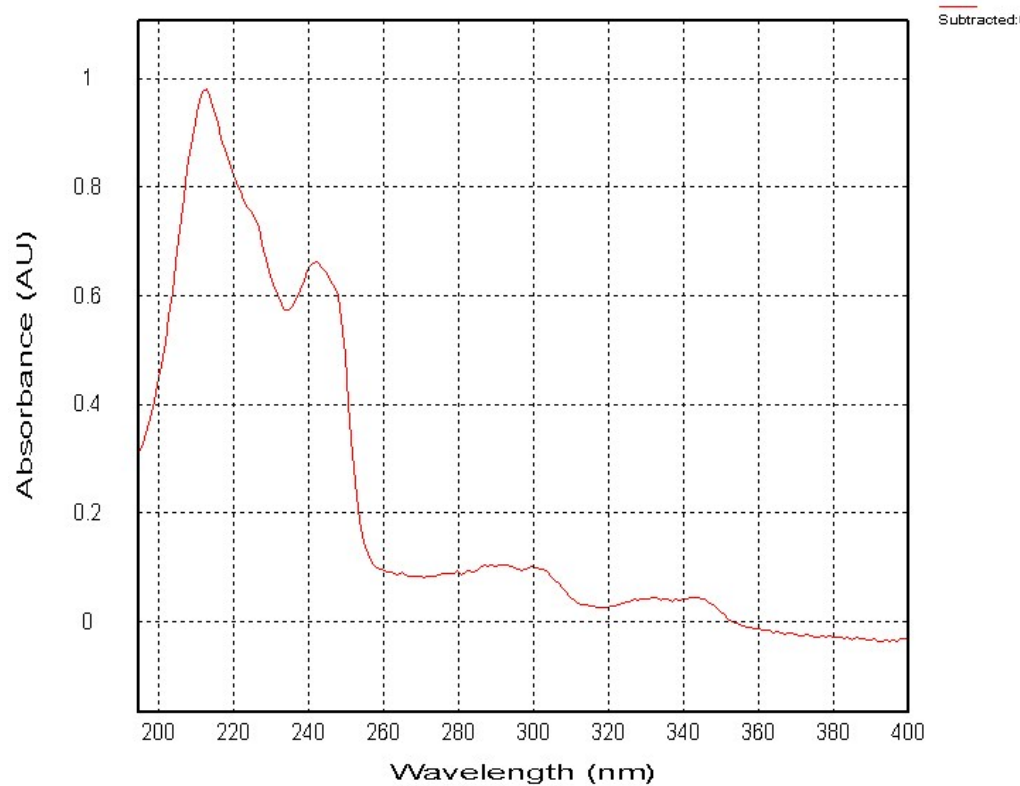


Fig. S37 UV spectrum of (-)-pratensilin C ((-)-3).

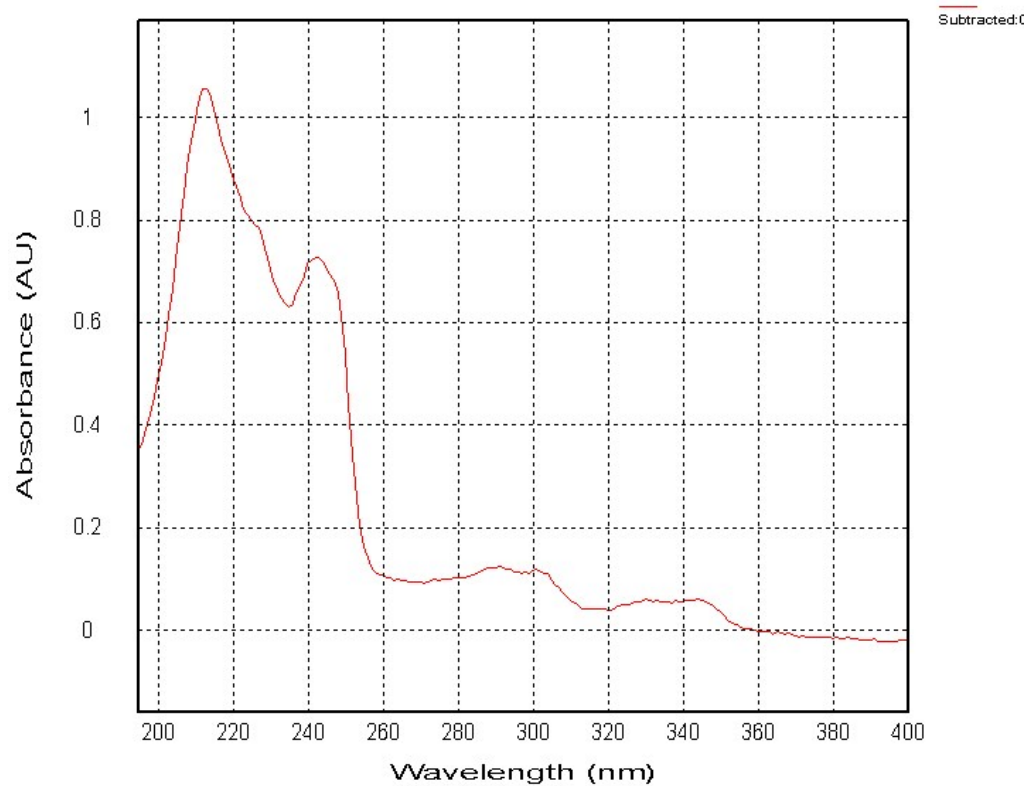


Fig. S38 IR spectrum of (\pm)-pratensilin C (3).

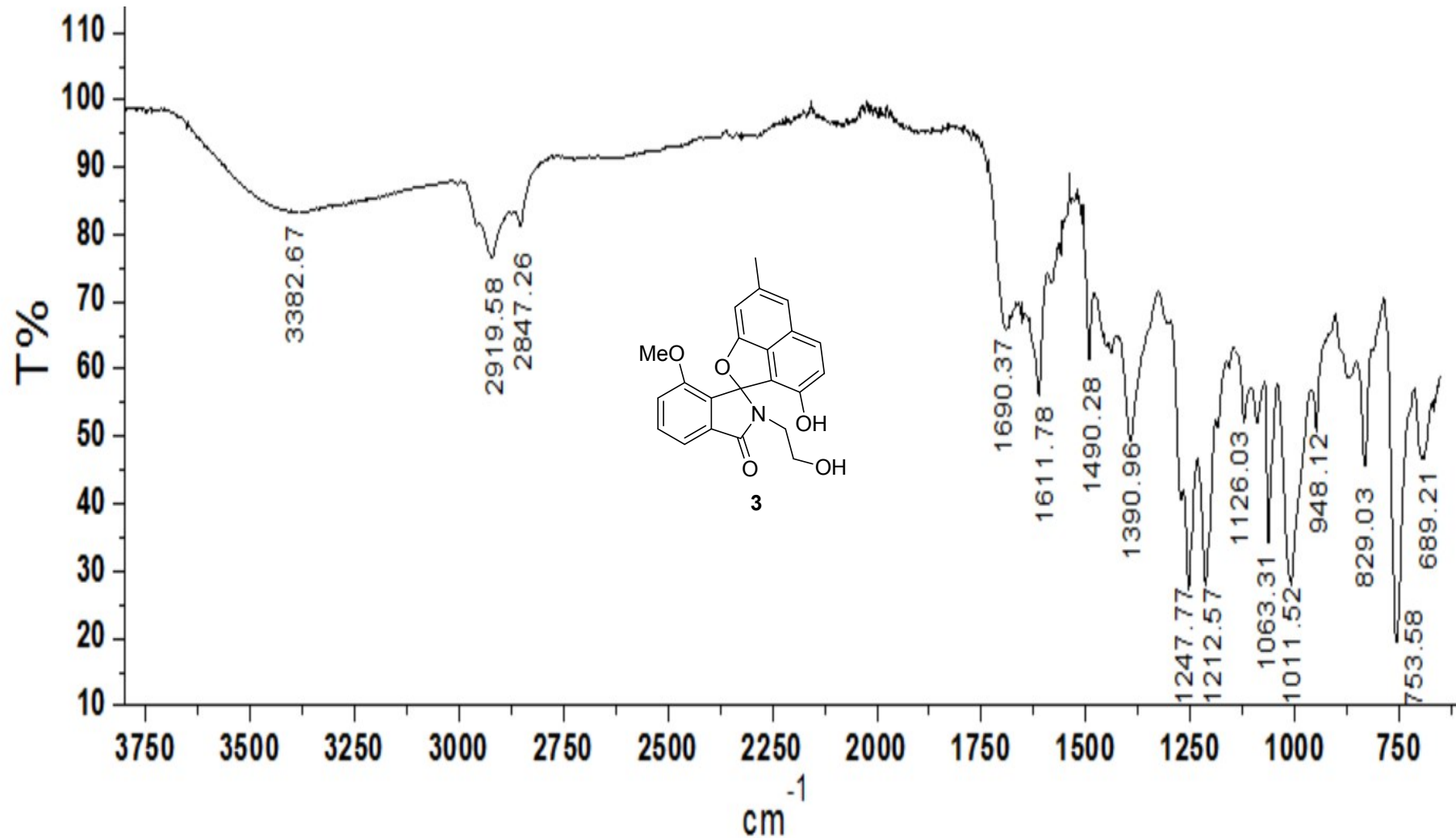


Fig. S39 ^1H NMR spectrum (500 MHz) of (\pm)-methy pratensilin B (**4**) in $\text{DMSO}-d_6$.

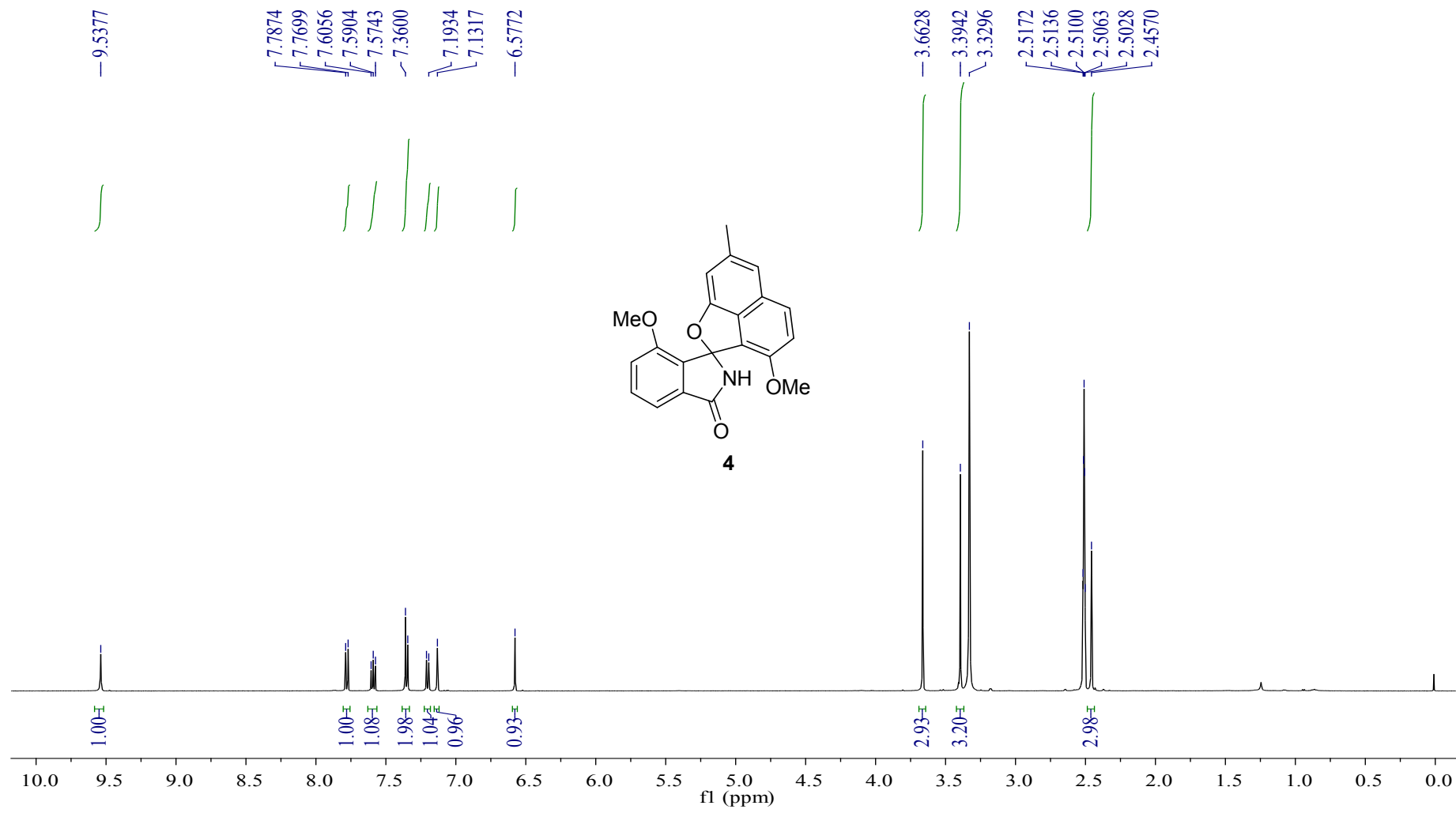


Fig. S40 ^{13}C NMR spectrum (125 MHz) of (\pm)-methy pratensilin B (**4**) in $\text{DMSO}-d_6$.

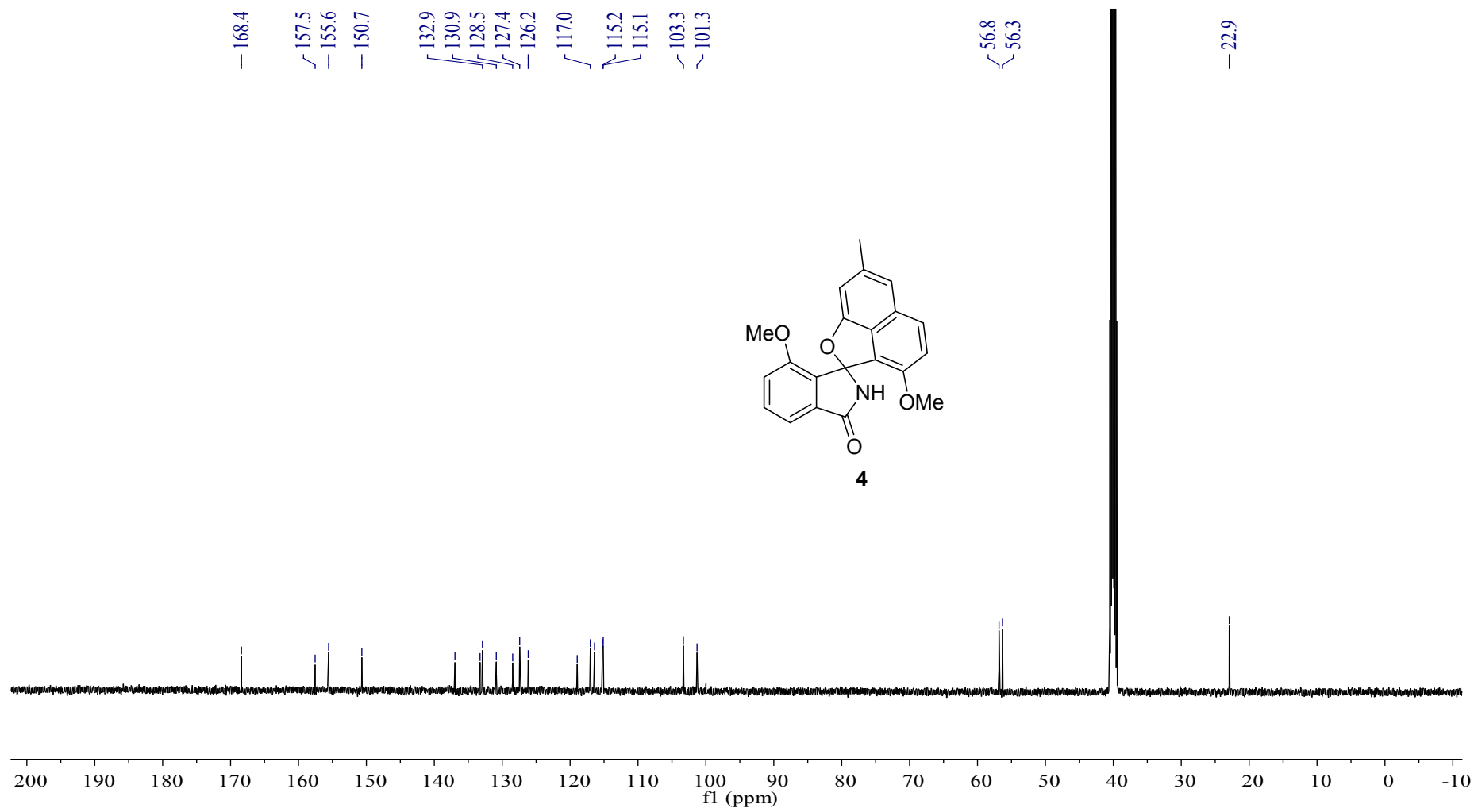


Fig. S41 ESIMS spectrum of (\pm)-methy pratensilin B (**4**).

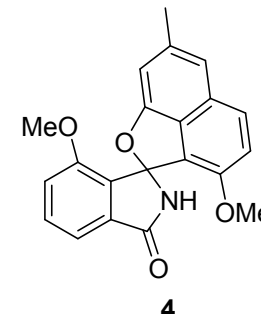
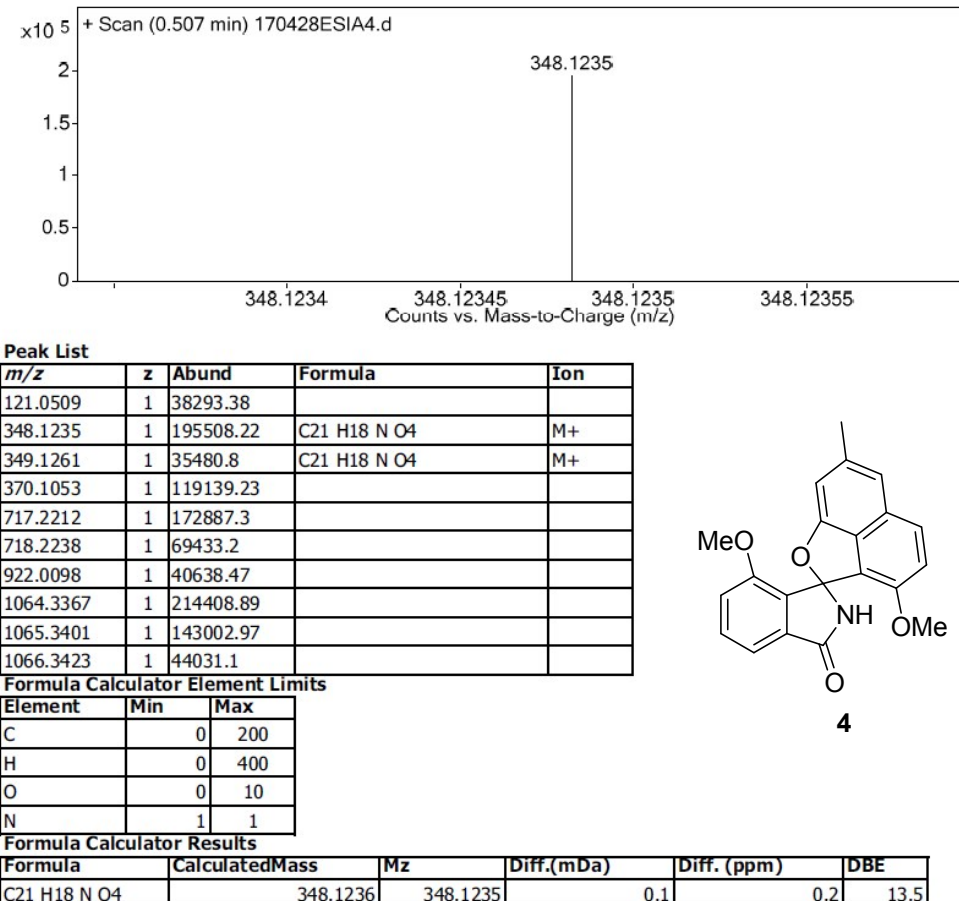


Fig. S42 UV spectrum of (+)-methy pratensilin B ((+)-4).

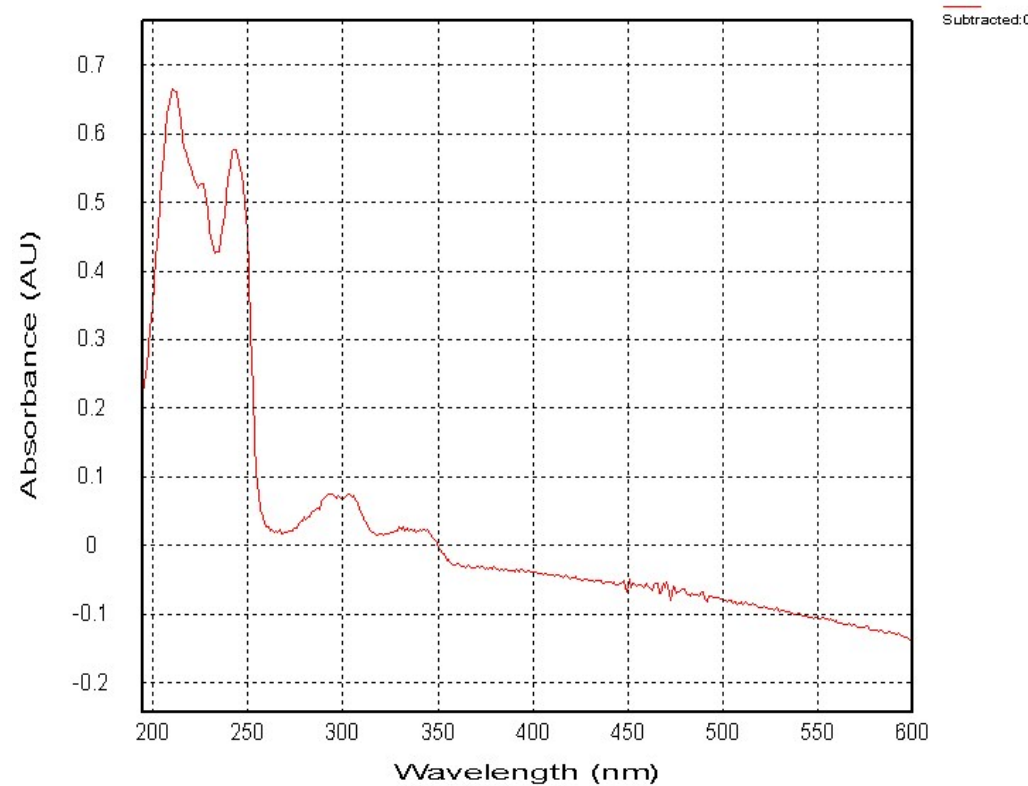


Fig. S43 UV spectrum of (-)-methy pratensilin B ((-)-4).

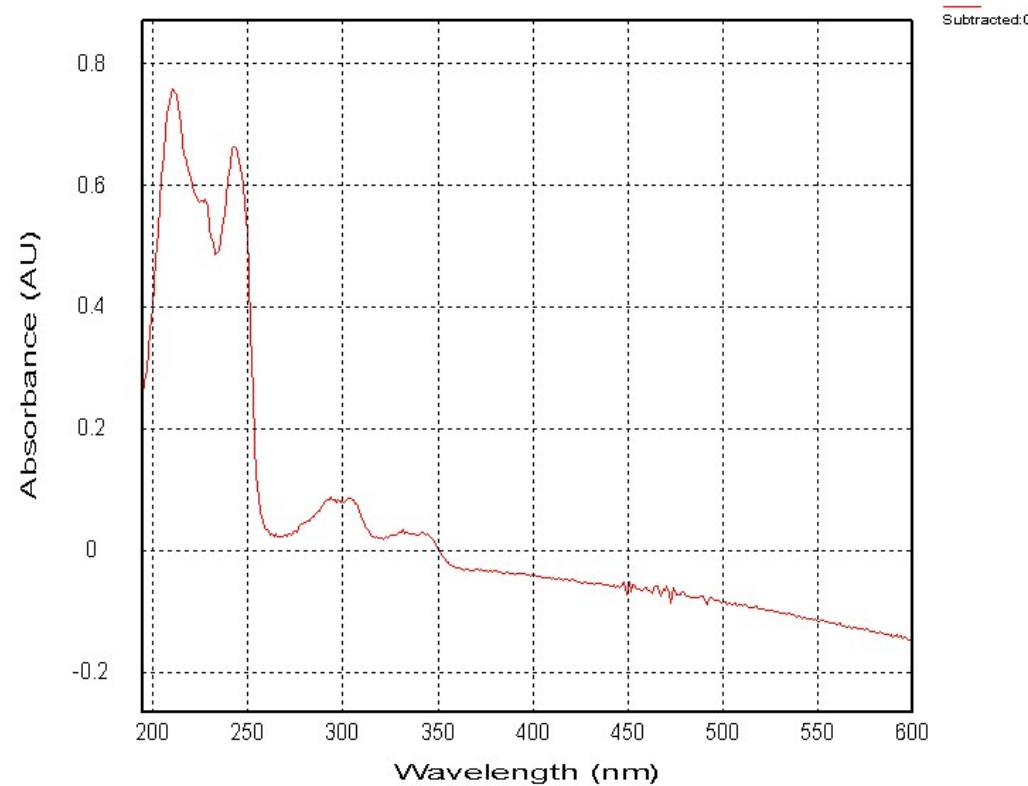


Fig. S44 ^1H NMR spectrum (500 MHz) of 8-*O*-methylrabelomycin in CDCl_3 .

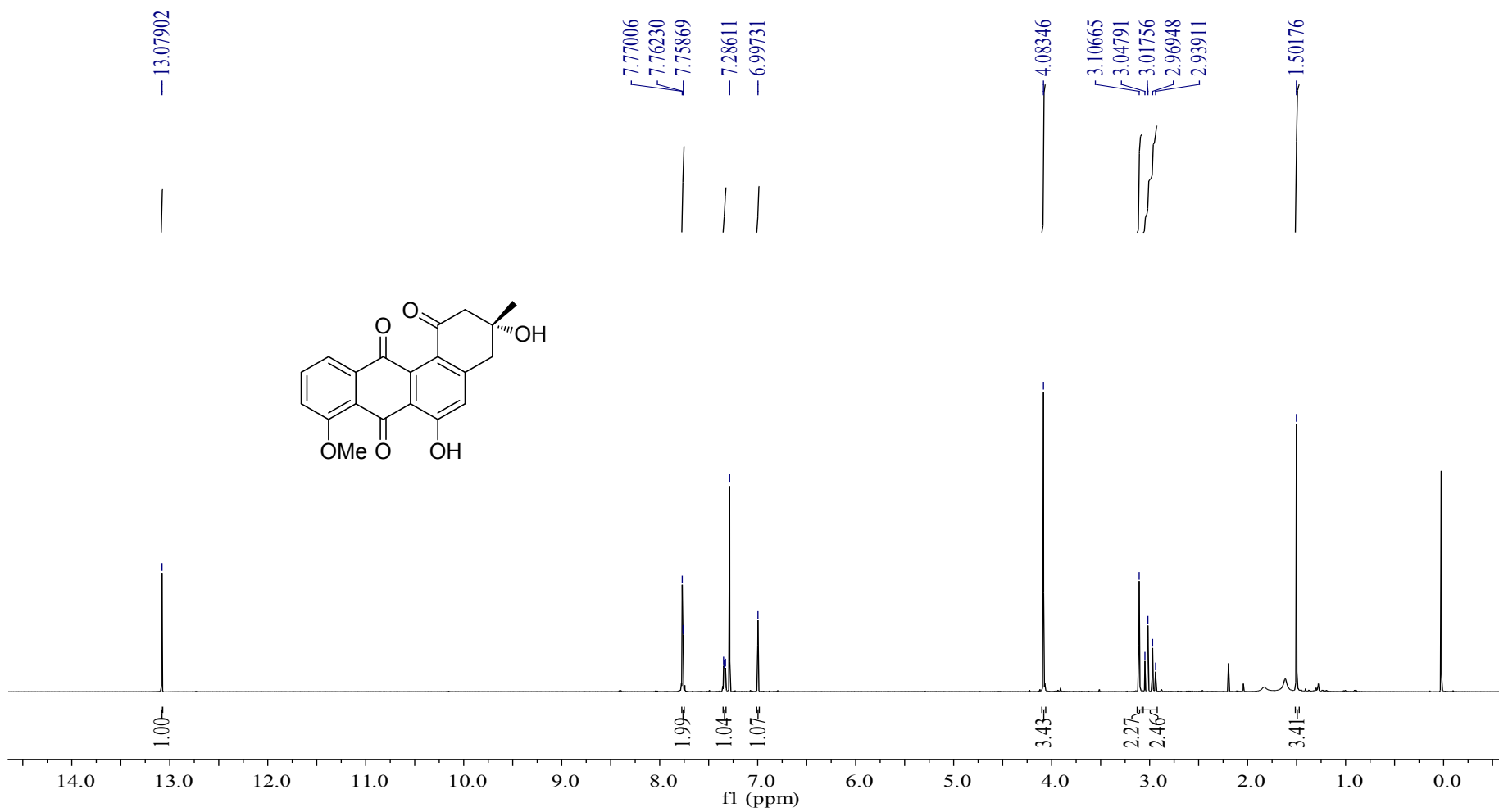


Fig. S45 ^{13}C NMR spectrum (125 MHz) of 8-*O*-methylrabelomycin in CDCl_3 .

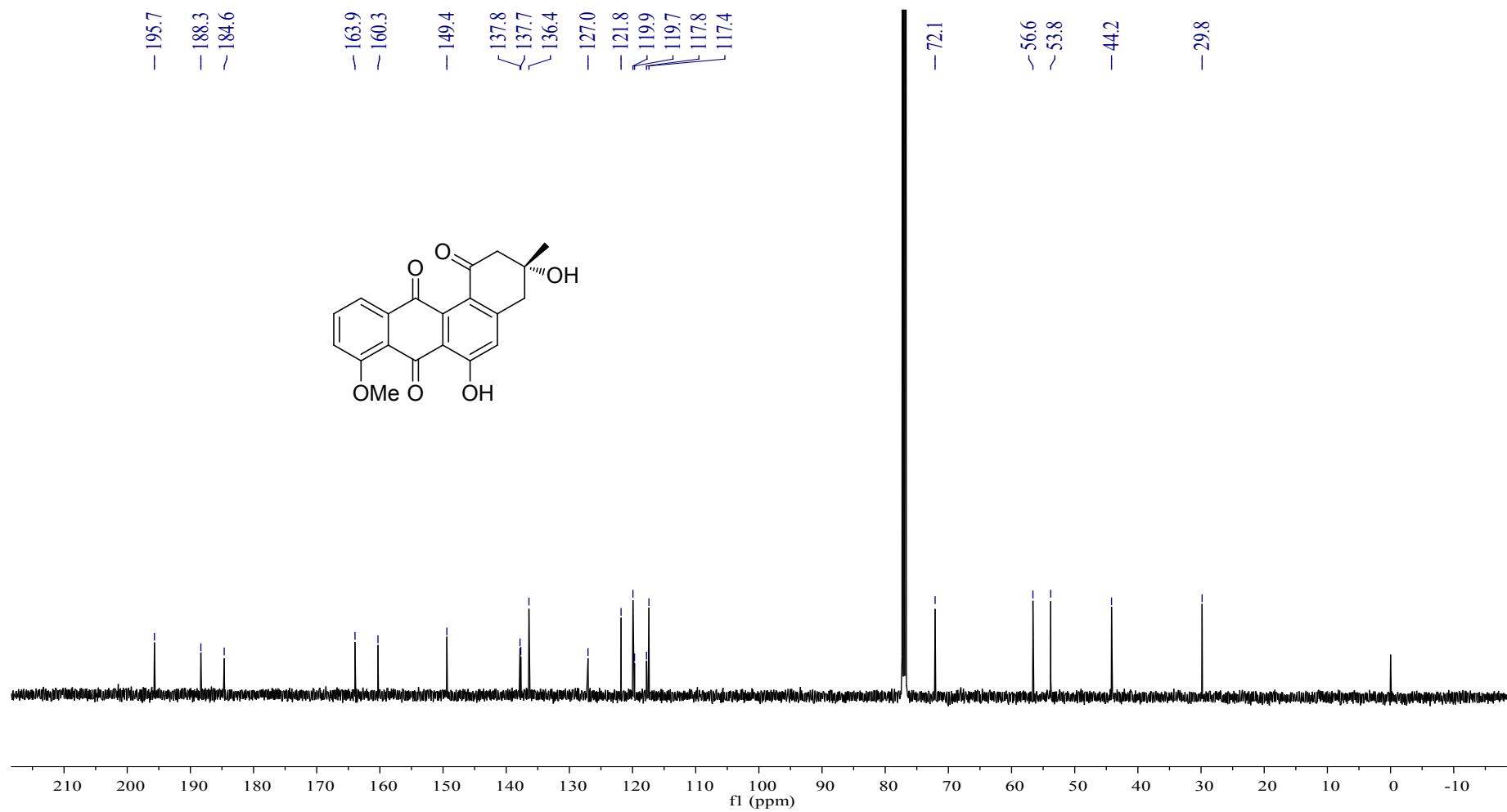
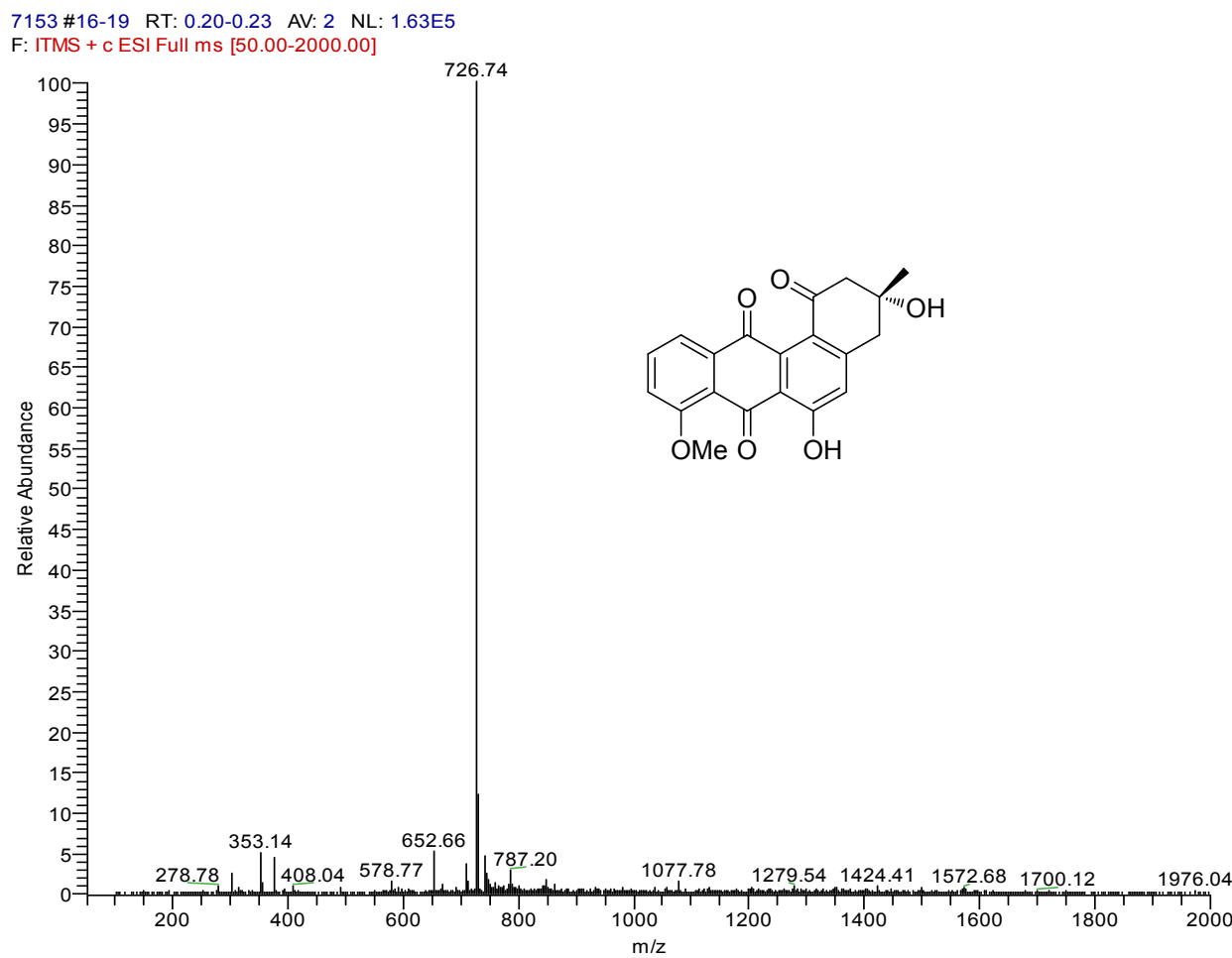


Fig. S46 ESIMS spectrum of 8-*O*-methylrabelomycin.



X-ray crystallographic analysis of (\pm)-pratensilins A (1). X-ray quality crystals were acquired by slow volatilization of a solvent mixture of MeOH and CH₂Cl₂. Crystal data for cu_xzp_r714_0m: 2(C₂₀H₁₅NO₄)•H₂O, M = 684.68, triclinic, *a* = 8.5611(2) Å, *b* = 11.5649(3) Å, *c* = 17.2271(5) Å, α = 94.1390(10) $^\circ$, β = 95.1400(10) $^\circ$, γ = 109.6890(10) $^\circ$, *V* = 1589.89(7) Å³, *T* = 100(2) K, space group *P*-1, Z = 2, $\mu(\text{CuK}\alpha)$ = 0.843 mm⁻¹, 24293 reflections measured, 5373 independent reflections (*R*_{int} = 0.0337). The final *R*_I values were 0.0366 (*I* > 2 σ (*I*)). The final *wR*(*F*²) values were 0.0943 (*I* > 2 σ (*I*)). The final *R*_I values were 0.0384 (all data). The final *wR*(*F*²) values were 0.0961 (all data). The goodness of fit on *F*² was 1.020. Crystallographic data for compound **1** has been deposited in the Cambridge Crystallographic Data Centre with deposition numbers CCDC 1474259.

Table S5. Crystal data and structure refinement for (\pm)-pratensilins A (1)

Identification code	cu_xzp_r714_0m
Empirical formula	C ₄₀ H ₃₂ N ₂ O ₉
Formula weight	684.68
Temperature	100(2) K
Wavelength	1.54178 Å
Crystal system, space group	Triclinic, P-1
Unit cell dimensions	<i>a</i> = 8.5611(2) Å alpha = 94.1390(10) deg. <i>b</i> = 11.5649(3) Å beta = 95.1400(10) deg. <i>c</i> = 17.2271(5) Å gamma = 109.6890(10) deg.
Volume	1589.89(7) Å ³
Z, Calculated density	2, 1.430 Mg/m ³
Absorption coefficient	0.843 mm ⁻¹

F(000)	716
Crystal size	0.20 x 0.15 x 0.06 mm ³
Theta range for data collection	2.59 to 66.99 deg.
Limiting indices	-10<=h<=10, -13<=k<=13, -20<=l<=19
Reflections collected / unique	24293 / 5373 [R(int) = 0.0337]
Completeness to theta = 66.99	94.6 %
Absorption correction	Semi-empirical from equivalents
Max. and min. transmission	0.9512 and 0.8496
Refinement method	Full-matrix least-squares on F ²
Data / restraints / parameters	5373 / 3 / 472
Goodness-of-fit on F ²	1.020
Final R indices [I>2sigma(I)]	R1 = 0.0366, wR2 = 0.0943
R indices (all data)	R1 = 0.0384, wR2 = 0.0961
Largest diff. peak and hole	0.268 and -0.250 e. Å

X-ray crystallographic analysis of (\pm)-pratensilins B (2). X-ray quality crystals were acquired by slow volatilization of a solvent mixture of MeOH and CH₂Cl₂. Crystal data for cu_xzp_r8631_0m: C₂₀H₁₅NO₄, $M = 333.33$, $a = 12.3534(2)$ Å, $b = 12.5563(2)$ Å, $c = 20.7245(4)$ Å, $\alpha = 90^\circ$, $\beta = 98.7570(10)^\circ$, $\gamma = 90^\circ$, $V = 3177.17(10)$ Å³, $T = 100(2)$ K, space group P21/c, $Z = 8$, $\mu(\text{CuK}\alpha) = 0.805$ mm⁻¹, 22703 reflections measured, 4413 independent reflections ($R_{\text{int}} = 0.1162$). The final R_I values were 0.0997 ($I > 2\sigma(I)$). The final $wR(F^2)$ values were 0.2435 ($I > 2\sigma(I)$). The final R_I values were 0.1606 (all data). The final $wR(F^2)$ values were 0.3106 (all data). The goodness of fit on F^2 was 1.112. . Crystallographic data for compound 2 has been deposited in the Cambridge Crystallographic Data Centre with deposition numbers CCDC

1557858.

Table S6. Crystal data and structure refinement for (\pm)-pratensilins B (2)

Identification code	cu_xzp_r8631_0m
Empirical formula	C ₂₀ H ₁₅ NO ₄
Formula weight	333.33
Temperature	100(2) K
Wavelength	1.54178 Å
Crystal system	Monoclinic
space group	P2 ₁ /c
Unit cell dimensions	a = 12.3534(2) Å $\square\alpha=90^\circ$. b = 12.5563(2) Å $\square\beta=98.7570(10)^\circ$. c = 20.7245(4) Å $\square\gamma=90^\circ$.
Volume	3177.17(10) Å ³
Z	8
Calculated density	1.394 Mg/m ³
Absorption coefficient	0.805 mm ⁻¹
F(000)	1392
Crystal size	0.220 x 0.220 x 0.060 mm ³
Theta range for data collection	6.048 to 58.089°.
Limiting indices	-13≤h≤13, -13≤k≤13, -22≤l≤20
Reflections collected	22703

Independent reflections	4413 [R(int) = 0.1162]
Completeness to theta = 58.089°	99.1 %
Absorption correction	Semi-empirical from equivalents
Refinement method	Full-matrix least-squares on F ²
Data / restraints / parameters	4413 / 12 / 458
Goodness-of-fit on F ²	1.112
Final R indices [I>2sigma(I)]	R1 = 0.0997, wR2 = 0.2435
R indices (all data)	R1 = 0.1606, wR2 = 0.3106
Largest diff. peak and hole	0.515 and -0.578 e.Å ⁻³

X-ray crystallographic analysis of (\pm)-pratensilins C (3). X-ray quality crystals were acquired by slow volatilization of a solvent mixture of MeOH and CH₂Cl₂. Crystal data for cu_xzp_r8629_0m: 4(C₂₂H₁₉NO₅)•CH₄O, $M = 1541.57$, $a = 12.3247(13)$ Å, $b = 12.4856(12)$ Å, $c = 13.5866(14)$ Å, $\alpha = 82.066(2)^\circ$, $\beta = 75.198(3)^\circ$, $\gamma = 70.107(3)^\circ$, $V = 1897.7(3)$ Å³, $T = 100(2)$ K, space group P-1, $Z = 1$, $\mu(\text{CuK}\alpha) = 0.797$ mm⁻¹, 23992 reflections measured, 6743 independent reflections ($R_{int} = 0.0507$). The final R_I values were 0.0566 ($I > 2\sigma(I)$). The final $wR(F^2)$ values were 0.1654 ($I > 2\sigma(I)$). The final R_I values were 0.0582 (all data). The final $wR(F^2)$ values were 0.1674 (all data). The goodness of fit on F^2 was 1.032. Crystallographic data for compound 3 has been deposited in the Cambridge Crystallographic Data Centre with deposition numbers CCDC 1557874.

Table S7. Crystal data and structure refinement for (\pm)-pratensilins C (3)

Identification code	cu_xzp_r8629_0m
Empirical formula	C ₈₉ H ₈₀ N ₄ O ₂₁
Formula weight	1541.57
Temperature	100(2) K
Wavelength	1.54178 Å
Crystal system	Triclinic
space group	<i>P</i> -1
Unit cell dimensions	a = 12.3247(13) Å $\square\alpha=82.066(2)^\circ$. b = 12.4856(12) Å $\square\beta=75.198(3)^\circ$. c = 13.5866(14) Å $\square\gamma=70.107(3)^\circ$.
Volume	1897.7(3) Å ³
Z	1
Calculated density	1.349 Mg/m ³
Absorption coefficient	0.797 mm ⁻¹
F(000)	810
Crystal size	0.550 x 0.440 x 0.270 mm ³
Theta range for data collection	3.370 to 70.493°.
Limiting indices	-14≤=h≤=14, -14≤=k≤=15, -16≤=l≤=16
Reflections collected	23992
Independent reflections	6743 [R(int) = 0.0507]
Completeness to theta = 67.679°	95.1 %

Absorption correction	Semi-empirical from equivalents
Refinement method	Full-matrix least-squares on F^2
Data / restraints / parameters	6743 / 0 / 534
Goodness-of-fit on F^2	1.032
Final R indices [$I > 2\sigma(I)$]	$R_1 = 0.0566$, $wR_2 = 0.1654$
R indices (all data)	$R_1 = 0.0582$, $wR_2 = 0.1674$
Extinction coefficient	0.0042(5)
Largest diff. peak and hole	0.572 and -0.306 e. \AA^{-3}
